Universidad Carlos III de Madrid

BACHELOR'S THESIS

University Degree in Aerospace Engineering

# Analysis of composite laminate plates subjected to ballistic impact

**Alberto Rodríguez Amor**

*Tutor*

**Jose Alfonso Artero Guerrero**

June 2019

# Abstract

During many years and still nowadays, ballistic impacts are an important field of study. In a world in which every year the air transport demand increases linearly, major aerospace companies focus their efforts in developing the next generation of aircrats with materials harder and resistant to almost any type of impact, making them also aerodynamically more efficient and the most lightweight as possible. And those materials that are fulfilling those requirements and still have enough potential to success are composite materials.

The main objective of this paper is to describe in detail the analysis performed to a composite laminate plate which is subjected to different ballistic impacts.

By doing this and for the ease of comprehension, the project will be divided into several parts. Firstly it will be described what is and how behaves a composite material and specifically the type used for this analysis which is a laminate composite.

To perform the ballistic process, the computational finite element program LS-Dyna® will be utilized to model all the scenarios subjected to analyze. However, before doing the expected cases, it will be described a sensitivity analysis in which all the features and tools used to generate an efficient and realistic ballistic impact will be introduced. Several trials will be evaluated and compared with experimental data to select the best case which will be used onwards on the project.

After that, the cases to be analyzed will be described. The selected laminate composite plate will be subjected to a variation in geometry, thickness, boundary conditions and mechanical properties under the same type of ballistic impacts. The analysis of the results will be based on one important failure mode which is crucial in the analysis of composite materials, the delamination produced. Moreover, it will be studied also the residual velocity displayed after the impact.

Finally, last chapters of the project will be devoted to the regulatory framework involved throughout this analysis, the socio-economic impact that this type of study and analysis of composite materials provokes in the real life and the estimation of the budget that this project would generate.

**Keywords:** composite, material, laminate plate, impact, delamination, residual velocity, delaminated area

## Acknowledgements

Before starting with the thesis, I would like to write a few words devoted to those people who have been there throughout the whole degree and also during the realization of this thesis.

This project represents the culminating point of these four years of hard and difficult work and study, a full stop for this period but also the starting point for new pages to be written.

I would like to thank my parents very much for their unconditional support during this time, visiting me in Madrid and Bristol, helping me and encouraging me every time I needed and even when I do not realize of that. I have enjoyed a lot this year coming home again with you since 4 years abroad. This project is also yours.

I would also say a special thank you to Natalia, for being there in those tough moments of the degree, giving me the boost to continue working and studying, and also for her love, happiness and support.

Of course, I would like to thank Jose for giving me the chance to make this project, offering me this interesting topic and be there solving my doubts and giving me guidance and tips in order to make a good and professional thesis.

I cannot forget also the rest of my family, above all my uncle Juanjo; thanks to leave me live with you this year in Madrid, and giving me everything I need and more during the degree and also for visiting me in Bristol.

Thanks to all my friends both in the residence of Leganés that I will remember them forever and also my friends in Zamora, specially Germán and Pedro. My Quintana´s neighbour Kike, enjoying this last special year together. Thanks Flavia, Juan, Elena, Manu, Cristóbal, Mercedes and Mikel for those funny moments, laughs and great memories.

Finally, thanks to all the professors and teachers that have taught me during my academic life. The ones in my school in Zamora since with them I could arrive to this great university, Universidad Carlos III the Madrid, and also the ones during the whole degree both in Madrid and Bristol. I will try to remember all your knowledge, teachings and values.

# Contents


Page

**1 Introduction** **1**
- 1.1 Motivation . . . 1
- 1.2 Scope of the project . . . 3
- 1.3 Basic concepts about composite materials . . . 3
  - 1.3.1 Laminate composite plates . . . 5
  - 1.3.2 Impacts on laminate composite plates . . . 8
  - 1.3.3 Failure modes on laminate composite plates . . . 9

**2 State of the art** **11**

**3 Methodology** **13**
- 3.1 Experimental test . . . 13
- 3.2 Introduction to LS-Dyna® . . . 14
- 3.3 Composite laminate plate modelling . . . 15
- 3.4 Validation . . . 20
- 3.5 Cases subjected to analysis . . . 29
  - 3.5.1 Variation of the laminate plate dimensions . . . 29
  - 3.5.2 Variation of the laminate plate thickness . . . 30
  - 3.5.3 Variation of the laminate boundary conditions . . . 30
  - 3.5.4 Variation of the laminate plate mechanical properties . . . 31

**4 Results and discussions** **32**
- 4.1 Effect of dimensional variation . . . 32
- 4.2 Effect of thickness variation . . . 35
- 4.3 Effect of boundary condition variation . . . 37
- 4.4 Effect of material property variation . . . 39

**5 Regulatory framework** **43**

**6 Socio-economic environment** **44**
- 6.1 Socio-economic impact . . . 44
- 6.2 Project budget . . . 45

**7 Conclusions** **47**
- 7.1 Final conclusions . . . 47
- 7.2 Future work . . . 48

**References** **49**

**Appendix A - Ballistic impact modelling code of LS-Dyna®** **I**

**Appendix B - 55x110 mm laminate plate** **XII**

**Appendix C - 110x110 mm laminate plate** XIII

**Appendix D - 165x110 mm laminate plate** XIV

**Appendix E - Gantt Chart** XV

# List of Figures


1 Forecast of annual air transport in terms of RPK in billions [1] . . . . 1
2 Structural composition of the B-787 [2] . . . . . . . . . . . . . . . . . 2
3 Laminate of woven fabric [8] . . . . . . . . . . . . . . . . . . . . . . . 4
4 Classification of composites according to reinforcements [7] . . . . . . 5
5 Types of laminate plates depending on the staking sequence [8] . . . . 6
6 Stacking sequence of the analysis . . . . . . . . . . . . . . . . . . . . 7
7 Impact on airplane nose [12] . . . . . . . . . . . . . . . . . . . . . . . 8
8 Impact on Leading Edge [12] . . . . . . . . . . . . . . . . . . . . . . . 8
9 Delamination due to matrix cracking [14] . . . . . . . . . . . . . . . . 9
10 Failure modes [9] . . . . . . . . . . . . . . . . . . . . . . . . . . . . . 10
11 First aircraft using composites in WWII . . . . . . . . . . . . . . . . 11
12 A350-1000 [3] . . . . . . . . . . . . . . . . . . . . . . . . . . . . . . . 12
13 Canyon scheme [8] . . . . . . . . . . . . . . . . . . . . . . . . . . . . 13
14 Pneumatic canyon pressurized with light gas ($CO_2$ or He) [9] . . . . . 14
15 FEM of a ballistic impact by LS-Dyna® . . . . . . . . . . . . . . . . 15
16 Element types [25] . . . . . . . . . . . . . . . . . . . . . . . . . . . . 16
17 Representation of the stresses involved and their directions . . . . . . 18
18 Bilinear traction-separation law [26] . . . . . . . . . . . . . . . . . . . 19
19 Mixed-mode traction-separation law for the cohesive element [26] . . 20
20 Delamination simulation by LS-Dyna® . . . . . . . . . . . . . . . . . 20
21 Comparison of residual velocities between the computational meshes and the experimental case . . . . . . . . . . . . . . . . . . . . . . . . 21
22 Comparison of delaminated area between the computational meshes and the experimental case . . . . . . . . . . . . . . . . . . . . . . . . 22
23 Cross sections of the projectiles . . . . . . . . . . . . . . . . . . . . . 24
24 Comparison of delaminated area between the sphere meshes and the experimental case . . . . . . . . . . . . . . . . . . . . . . . . . . . . 25
25 Comparison of residual velocities between the sphere meshes and the experimental case . . . . . . . . . . . . . . . . . . . . . . . . . . . . 26
26 Final residual velocity results . . . . . . . . . . . . . . . . . . . . . . 27
27 Final delaminated area results . . . . . . . . . . . . . . . . . . . . . . 27
28 Delamination pattern of the cohesive element between laminas at 45º and -45º respectively . . . . . . . . . . . . . . . . . . . . . . . . . . 28
29 Delamination pattern of the cohesive element between laminas at 0º and 90º respectively . . . . . . . . . . . . . . . . . . . . . . . . . . . 29
30 Stacking sequence of the 12-lamina plate . . . . . . . . . . . . . . . . 30
31 Zoom in at all nodes clamped (left) and at the bottom lamina nodes clamped (right) . . . . . . . . . . . . . . . . . . . . . . . . . . . . . . 31
32 Comparison of delaminated area between the original case and the quadrangular variations . . . . . . . . . . . . . . . . . . . . . . . . . 32
33 Comparison of residual velocities between the original case and the quadrangular variations . . . . . . . . . . . . . . . . . . . . . . . . . 33

34 Comparison of delaminated area between the original case and the rectangular variations . . . . . . . . . . . . . . . . . . . . . . . . . . . 34
35 Comparison of residual velocities between the original case and the rectangular variations . . . . . . . . . . . . . . . . . . . . . . . . . . . 35
36 Comparison of delaminated area between plates with different thickness 36
37 Comparison of residual velocities between plates with different thickness 36
38 Comparison of delaminated area between plates with different bc´s . 37
39 Comparison of residual velocities between plates with different bc´s . 38
40 Comparison of delaminated area between plates with different mechanical properties . . . . . . . . . . . . . . . . . . . . . . . . . . . 39
41 Comparison of delaminated area between plates with different mechanical properties . . . . . . . . . . . . . . . . . . . . . . . . . . . 40
42 Comparison of residual velocities between plates with different mechanical properties . . . . . . . . . . . . . . . . . . . . . . . . . . . 41
43 Comparison of residual velocities between plates with different mechanical properties . . . . . . . . . . . . . . . . . . . . . . . . . . . 42

# List of Tables


1 AS4-8552 mechanical properties [11] . . . . . . . . . . . . . . . . . . . . 7
2 Projectile material properties . . . . . . . . . . . . . . . . . . . . . . . . . 16
3 Parameters for the cohesive interaction model . . . . . . . . . . . . . . 18
4 Divisions of the laminate plate meshes analysed . . . . . . . . . . . . 21
5 Values of residual velocities and deviations for the cases analysed . . 23
6 Values of delaminated area and deviations for the cases analyzed . . . 23
7 Sphere types considered . . . . . . . . . . . . . . . . . . . . . . . . . . 24
8 New property values . . . . . . . . . . . . . . . . . . . . . . . . . . . . 31
9 Segregated costs and expenses of the total budget . . . . . . . . . . . 46

## List of abbreviations 1

| **Symbols** | Meaning |
|---|---|
| $\rho_f$ | Fibre density |
| $\rho_m$ | Matrix density |
| $\rho_c$ | Composite density |
| $E_1$ | Longitudinal Young´s modulus |
| $\chi_c$ | Longitudinal compressive strength |
| $\chi_t$ | Longitudinal tensile strength |
| $E_2$ | Transverse Young´s modulus |
| $\Upsilon_c$ | Transverse compressive strength |
| $\Upsilon_t$ | Transverse tensile strength |
| $\mathbf{S}$ | In-plane shear strength |
| $\upsilon_{12}$ | Poisson´s ratio in direction 12 |
| $\upsilon_{21}$ | Poisson´s ratio in direction 21 |
| $\rho_s$ | Steel density |
| $E_s$ | Steel Young´s modulus |
| $\upsilon_s$ | Steel Poisson´s ratio |
| $\mathbf{T}$ | Peak traction in normal direction |
| $\boldsymbol{S}$ | Peak traction in tangential direction |
| $\mathbf{G}_I$ | Energy release rate for mode I (normal) |
| $\mathbf{G}_{II}$ | Energy release rate for mode II (tangential) |
| $\mathbf{u}_n$ | Ultimate displacement in normal direction |
| $\mathbf{u}_t$ | Ultimate displacement in tangential direction |
| $\delta_m$ | Mixed-mode total relative displacement |
| $\delta_I$ | Relative separation in normal direction |
| $\delta_{II}$ | Relative separation in tangential direction |

| **Symbols** | Meaning |
|---|---|
| $\delta^0$ | Initial Mixed-mode damage displacement |
| $\delta_I^0$ | Single mode damage initiation separation in normal direction |
| $\delta_{II}^0$ | Single mode damage initiation separation in tangential direction |
| $\delta^F$ | Ultimate Mixed-mode damage displacement |
| **kN** | Normal stiffness of the cohesive material |
| **kT** | Tangential stiffness of the cohesive material |
| $\beta$ | Mode mixity coefficient |
| $\alpha$ | B-K law coefficient |

## List of abbreviations 2

| **Acronym** | Stands for |
|---|---|
| **CAA** | Civil Aviation Authority |
| **CFRP** | Carbon Fibre Reinforced Polymer |
| **EASA** | European Aviation Safety Agency |
| **EU** | European Union |
| **FEA** | Finite Element Analysis |
| **FEM** | Finite Element Method |
| **HEDI** | High Energy Dynamic Impact |
| **NASA** | National Aeronautics and Space Administration |
| **RPK** | Revenue Passenger Kilometres |
| **USA** | United States of America |

# 1 Introduction

In this first section of the thesis several issues are going to be presented to the reader as introduction to the main work of the project. First of all the motivation that inspired the realization of the analysis of composite laminate plates; then, the objectives that will be accomplished by the end of the project and finally a resumed explanation of the structure and behaviour of composite materials subjected to impacts.

## 1.1 Motivation

Air transport has experimented during the last decades the major increase in volume of passengers and freight transportation among the rest means of transport. Moreover, important institutions and organizations of air transport have studied the prognosis over the next 10-20 years and all coincide in an increase of 5% annual rate. Obviously, these figures will be slightly different from the real ones, but the tendency will keep this optimistic behaviour even in the most pessimistic scenarios [1] .


Figure 1: Forecast of annual air transport in terms of RPK in billions [1]

Considering this increasing volume of air transport, large and low-cost airlines will decide to expand their fleet. Aircraft manufacturing companies will face this demand by making more sustainable, economic and efficient aircrafts. Nowadays, engineers are aware of improving the performance and endurance of airplanes by using lighter materials and reducing the fuel consumption. Many of the current fleets of airplanes already use a big amount of lightweight materials. Mainly, some parts of the airframe structure, fuselage and wings are made with composites but other important sections of the airplanes are still made of aluminium and titanium among other metals. Nevertheless, in the future, it is thought that the whole aircraft will be completely built by composite materials.

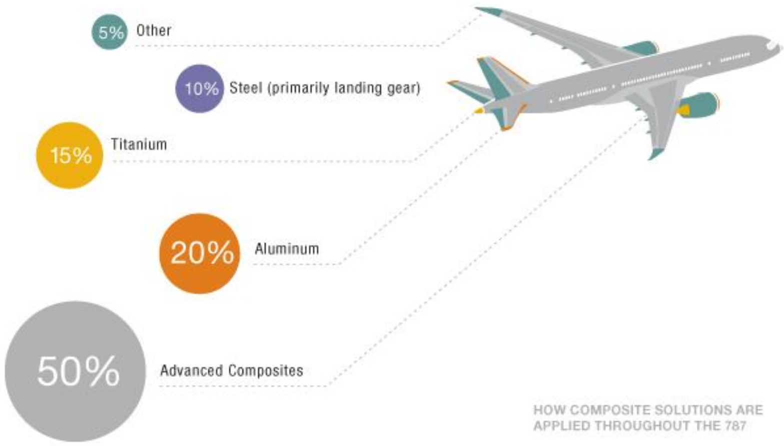


Figure 2: Structural composition of the B-787 [2]

Composite materials are those made by two or more constituent elements with different properties in such a way that the resultant material exhibits better mechanical, chemical and structural properties than the ones provided by each individual element separately. Carbon fibre is a well-known example of composite material in the airspace sector but there is a wide range of composite materials classified according to the type of fibre and matrix used (GFRP, aramid, Kevlar, epoxy. . . ) [3].

Fuselage and wings, both made of composites, of any type of aircraft either civil or military, are exposed during the flight and terminal flight phases to various impacts. Usually military aircrafts are the ones highly exposed to ballistic impact while performing manoeuvres in war zones [4]. Moreover, mid-air collisions are extremely dangerous due to the high speeds carried out by the airplanes. In both cases, important structural damages may be created and usually lead to fatal accidents. On the other hand, during terminal flight phases such as take-off, approach and landing, aircrafts may suffer any type of object impacts. Birds impacts are so common in the vicinity of the airdromes and airports and may lead to engine malfunctioning or shutdown due to the penetration into the turbine blades [5] . Also, little object impacts such as debris on the runway and taxiways provoke structural damage that must be inspected. Besides these cases, meteorological phenomena such as ice, hail, thunderstorm and turbulence can create also structural damages on the fuselage and wings. These are less dangerous than the previous cases but affect the aerodynamics and safety of the aircraft.

## 1.2 Scope of the project

The ultimate objective of this bachelor thesis is to know the behaviour and characteristics that laminate composite plates present when they are subjected to high velocity ballistic impacts and different conditions are applied. To reach this final aim, little chronological targets are set throughout this project:

- Elaborate a preliminary analysis. This will have huge importance since the configuration that better fits with the experimental data will be used onwards on the project. That real data will be extracted from the work made in the workshop of the University few years ago and with this project it will be validated. Computational modelling of several tests of laminate plates and projectiles are implemented in LS-Dyna®. Plates and projectiles in the shape of spheres are modelled varying the number of elements they are integrated. These trials are compared with the experimental data and discarded until the best one fits perfectly with the above mentioned in terms of delaminated area and residual velocity. A more detailed explanation will be displayed in the methodology section (chapter 3).
- Study the possible importance of changing the dimensions and thicknesses of the laminate plates with respect to base configuration. Longitudinal dimensions are varied making bigger and smaller quadrangular and rectangular plates and delaminated area is studied knowing if increases or decreases in these cases. Adding also more laminas, increases the thickness and its behaviour may determine the formulation of a relation that may connect thickness/delaminated area or thickness/residual velocity.
- Analyze the initial boundary conditions (simply supported through all the edges) of the original case and model other scenarios with different boundary conditions such as clamped through all the edges, simply supported and clamped just at the edges of the bottom lamina and free. With that, it will be shown which ones provide better conditions for avoiding delamination, or conversely whether they do not present any important difference.
- Change those mechanical properties of the material that predictably will have more influence on the failure process by analyzing the results of delamination. Furthermore, moreover by doing this, it will be also possible to determine which ones will make the laminate plate more resistant to ballistic impacts by modifying the values that the data sheet provides.

## 1.3 Basic concepts about composite materials

As explained in section 1.1, composite materials are composed by two or more materials called constituents which exhibits better properties together within the finished structure than any of the members alone can achieve [6]. This synergistic effect makes composites behave as anisotropic material since allows to enhance and tailor specific properties. There exist composite materials in nature such as wood or concrete, but this project is going to be based on the artificial composites made by humans and specially used in aerospace sector. Among the advantages that composite materials present, engineers seek for good mechanical properties, low weight, good fatigue performance and high chemical and corrosion resistance.

The principal constituents of composite materials are the reinforcement and the matrix. On one hand the reinforcement is all the material used to impart their special behaviour into the composite and according to the shape is integrated they can be classified as:

- **Particle**: dispersed phase, i.e. discrete or non-continuous phase constituent such as short globules or spheres made of metal, ceramic and plastic. They present good wear resistance, high stiffness and low cost since the manufacturing process is simple.
- **Fibre**: usually either short or long cylindrical constituent integrated as continuous and aligned fibres, discontinuous, (either aligned or randomly oriented) or woven fabric (see figure 3). Fibres are the most employed type of reinforcement due to the large stiffness and strength provided to the composite. Glass, carbon and aramid fibres are the most utilized materials [7].
- **Structural**: the most important characteristic is the geometry in which they are designed, and the properties of the materials employed. The most common examples of structural composites are laminates, which are pilling of layers called laminas of unidirectional composite materials, and sandwich panels, two external strong layers (face sheet) attached to a layer of less dense material (core) made of foam, polymer or honeycomb cells.

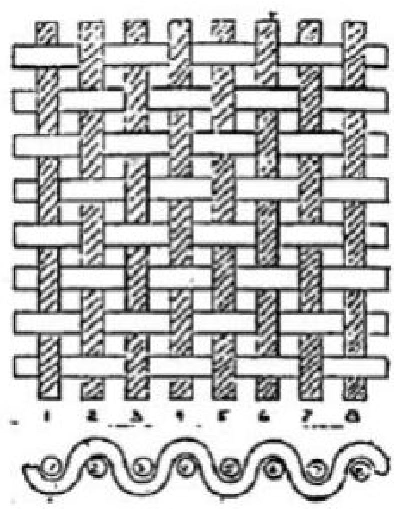

Figure 3: Laminate of woven fabric [8]

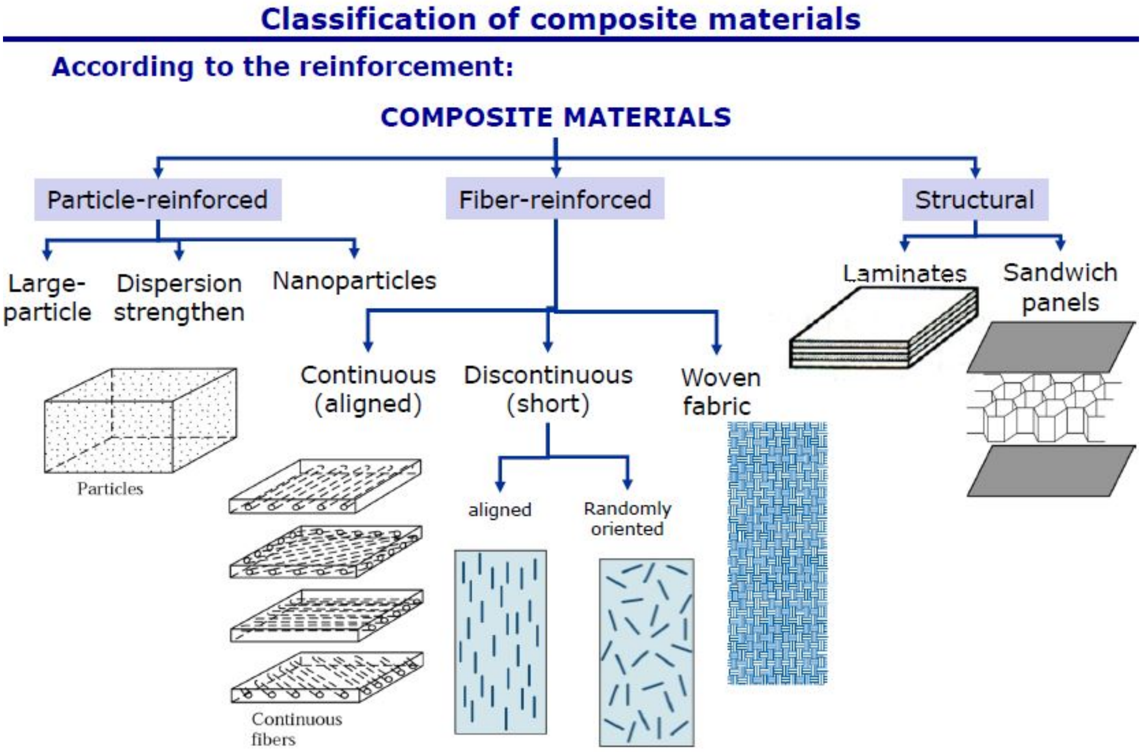


Figure 4: Classification of composites according to reinforcements [7]

On the other hand, the matrix is the part of the composite material that surrounds the other constituents. It provides protection to the fibres embedded and avoid corrosion and other problems associated to the exposure to adverse external environments that may affect the mechanical properties of the whole composite. Moreover, matrix exhibits large tenacity and ductility [9]. Depending of the material is made of, they are classified as metal, ceramic and polymeric matrix composites. Currently, epoxy matrix is the most used for aerospace applications. Among the properties it provides, is noticeable its easy processing, excellent chemical resistance and moisture absorption [10].

### 1.3.1 Laminate composite plates

Laminate composite plates can be manufactured using tapes of unidirectional carbon fibres pilling them in different angles or making a fabric of carbon fibres woven together. For this project, laminate composite plates with continuous carbon fibre reinforcement is selected. Generally, this type of structures, composed by several thin layers (laminas) is symmetric with respect to their middle plane and equilibrated to avoid anomalous distortions in the structure. Nevertheless, there exist more configurations of laminate plates such as antysimmetric or asymmetric depending on the required global character of the composite [7].

Fibre impregnation is the most common way to manufacture laminate plates for aerospace applications which require a versatile character to achieve the desired strength and stiffness. This resultant material, resin-impregnated fibre forms (*prepegs*), allows to control the mechanical properties by impregnating fibres changing their orientation with a controlled amount of resin (thermoset or thermoplastic), using solvent, hot-melt or powder-impregnation technologies [7] and stacking the laminas in a specific sequence for the required aerospace application.

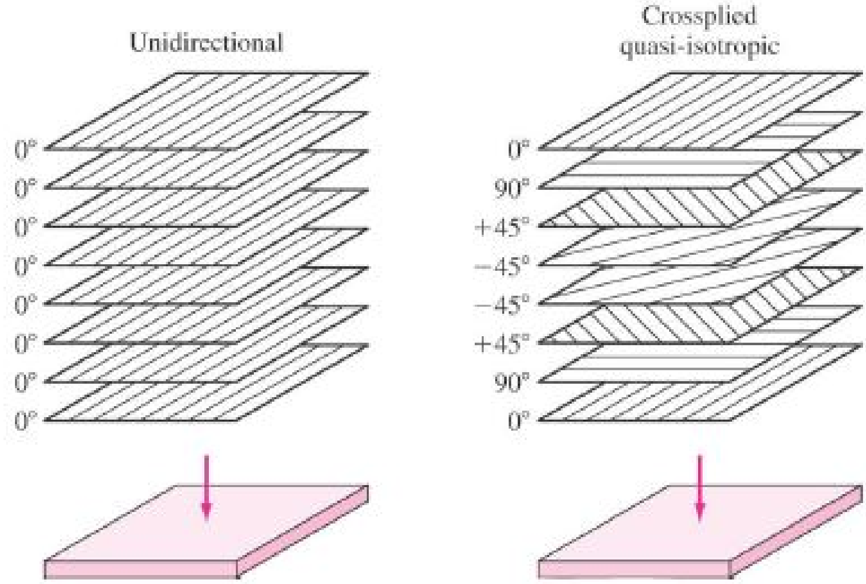


Figure 5: Types of laminate plates depending on the staking sequence [8]

Generally, laminate composites present orthotropic symmetry, mechanical properties of the fibres are designed to show their behaviour according to the direction in which they are oriented. The more laminas oriented to different angles, the more isotropic behaviour will have, i.e. the same value of the properties is found in all the directions. This last type of laminate composites are called quasi-isotropic.

HexPly® Prepeg AS4-8552 is the laminate composite utilized in the experimental analysis and manufactured by Hexcel®. This 110x110 mm plate is made of fibre carbon AS4 and epoxy 8552 exhibits high performance in primary aerospace structures [11]. Its good impact resistance and damage tolerance make this laminate a good choice for those parts exposes to crashes and impacts. The characteristic mechanical properties of the materials involved are resumed in Table 1 and will be introduced later in the computational modelling.

| Physical properties | | | |
|---|---|---|---|
| Fibre density, $\rho$f [kg/m3] | 1790 | Resin density, $\rho$m [kg/m3] | 1300 |
| Laminate thickness [mm] | 0.2 | Laminate density, $\rho$c[kg/m3] | 1580 |
| **Mechanical properties** | | | |
| $E_1 [Gpa]$ | 139 | $E_2 [Gpa]$ | 9 |
| $\chi_c [Mpa]$ | 1656 | $\chi_t [Mpa]$ | 2105 |
| $\Upsilon_c [Mpa]$ | 175 | $\Upsilon_t [Mpa]$ | 79 |
| S [Mpa] | 114 | $\upsilon_{12}$ | 0.3083 |

Table 1: AS4-8552 mechanical properties [11]

The stacking sequence of AS4-8552 selected in this project for performing the different cases to be analyzed is (+45/-45/0/90)s. This gives a total of 8 laminas with an overall thickness of 1.6 mm. In certain section, this sequence will be larger to study the behaviour under different circumstances with a thicker plate, but always maintaining the symmetry with respect to the middle plane.

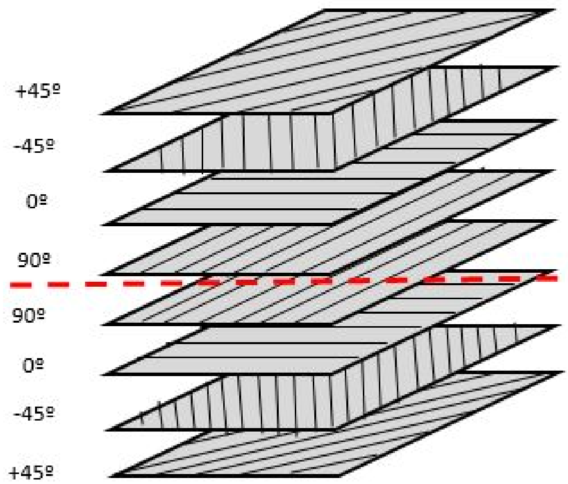


Figure 6: Stacking sequence of the analysis

On the other hand and before performing all the cases, an initial model made with the computational program selected for this project, will be validated with the experimental test. For doing that, the same scenario will be represented, with the same boundary conditions, properties and laminate plate. In this specific case, the model will have 12 laminas as in the real one with a sequence of (+45/-45/0/90/90/0)s. This will be explained in detail later on the project, within the subsection 3.1 in the methodology chapter.

### 1.3.2 Impacts on laminate composite plates

Laminate composite plates utilized on aeronautics, as it has been said previously at the beginning of the introduction, are susceptible to receive impacts during the whole operating lifetime. Obviously depending on the velocity with which an object hits the composite, it causes more or less damages. For the case of an airplane, it is not the same if a little object hits the panels of the wing while the aircraft is taxiing on the aprons or taxiways, that if it is on the air, approaching the airport, taking off or cruising. Thus, either little indentations or big penetrations can be produced. Velocity varies on these scenarios from 10-20 m/s to 200/300 m/s.

Figure 7: Impact on airplane nose [12]

Figure 8: Impact on Leading Edge [12]

It is widely accepted that low velocity impacts occur within a range of 1-10 m/s [13]. These impacts are present in the context of fall of big masses or tools, sometimes repeated on time, which can not get a high enough velocity and therefore do not create perforations on the surface but indentations which may affect the operating life of the material. Moreover, it affects the geometry and therefore the aerodynamics. Compression, shear and Rayleigh waves are created with the ballistic impact [14] and they are propagated through the laminate and stay residual for a time [15] and on the long-term provoke a global response of the structure affecting the geometry and the boundary conditions [16].

On the other hand, above that previous velocity range, high velocity impacts are considered. Although it depends on the characteristics of the material and the impactor, these velocities create cracks and perforations on the surfaces, leading to the failure of the composite material. If the projectile penetrates and goes through the composite plate, a residual velocity value is registered. This value will be studied throughout the different cases presented in this project.

### 1.3.3 Failure modes on laminate composite plates

Although the analysis performed in this project is based on high velocity impacts, low velocity impacts are extremely dangerous even though they may not create perforations but provoke the failure of the structure over time, as it have been mentioned recently.

Every part that composes the fuselage of the aircraft is perfectly polished to avoid turbulence and vortex that affect the aerodynamics. Therefore, indentations are seen perfectly and recognize with visual observation. However, internal damages are more difficult to determine and their identification is essential to know how they propagate through the material and what factors influence to preserve the integrity of the structure.

Two types of failure modes exists on these composites: intralaminar and interlaminar.

- **Interlaminar failure** is identify also as delamination and it is the detachment of adjacent laminas due to the propagation of cracks through the matrix. This was developed and described by Hull and Shi (1991) [17] who observed that these shear cracks provoke a displacement of the plies above the lamina that is detached [14].

  Several studies have stated that initiation and propagation of delamination cracks on edges follows modes I and II of interlaminar fracture mechanisms [18]. Moreover, it occurs between laminas with different orientations and the shape and size of the delaminated area is influenced by three factors: the difference between $E_1$ and $E_2$ of each lamina, the thickness of the lamina or group of laminas and the deflection of the laminate [19]. Delamination together with the residual velocity previously mentioned, will be the factors to be studied in the different cases analyzed throughout this project.

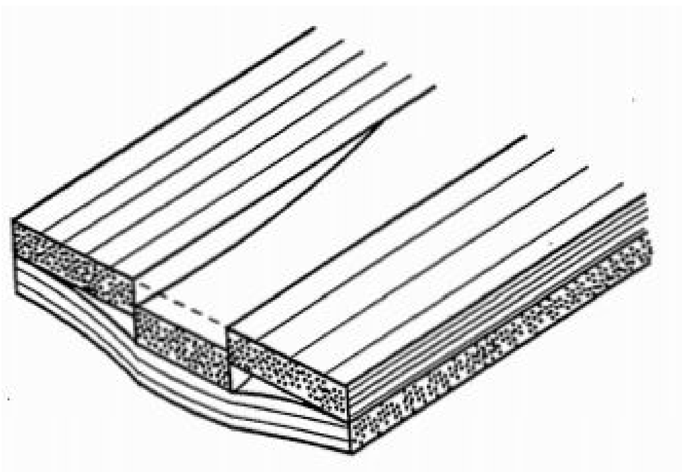

Figure 9: Delamination due to matrix cracking [14]

- **Intralaminar failure**, as the word itself indicates, is related to all those modes that occur inside the laminas. Matrix cracking is usually the first failure mode to appear due to the concentration of tension and shear stresses that create a little local flaws in the matrix which will be propagated with time [8].

  Fibre breakage is the other example of intralaminar failure due to the propagation of loads and cracks perpendicularly to the fibres orientation.Therefore, this breakage occurs after matrix cracking and interlaminar failure.

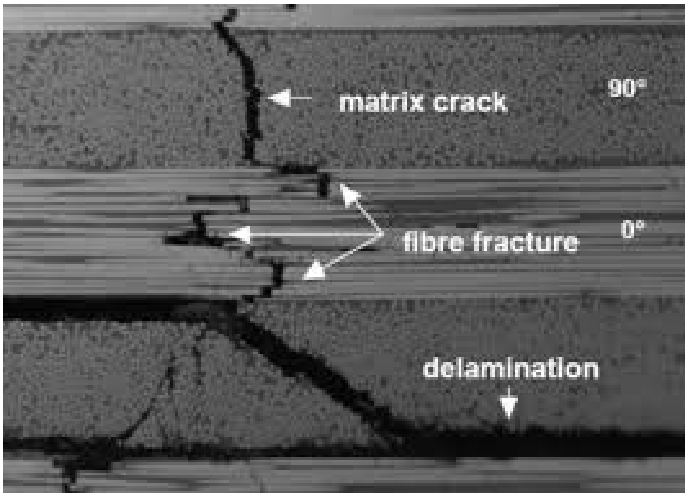


Figure 10: Failure modes [9]

# 2 State of the art

During the second half of the last century, composite materials have been studied and analyzed by many engineers and researchers, becoming so popular for many applications and structures, above all in the aerospace industry.

The development of plastics in the early 1900s led to the birth of modern composite materials. Until then, only natural resins obtained from plants and animals were used as glues and varnishes. Scientists realized that these new synthetic materials exhibited good mechanical properties for structural applications. Owens Corning introduced in 1935 the glasssfibre, beginning with the so called Fibre Reinforced Polymer industry [20].

As it occurs many times with wars, some of the developments and advances in composites were brought by World War II. Its principal application for military purposes not only showed great strength, lightweight and resistance, but also other characteristics that would be essential for winning the war like not being seen by electronic surveillance devices as it is the case of glassfibre.

Figure 11: First aircraft using composites in WWII

Brandt Goldsworthy, also known as "the grandfather of composites" extended the production of composite materials by developing new manufacturing process as the pultrusion. From 1950s on-wards, new composite materials were discovered. Roger Bacon created the carbon fibre composite, which would start replacing metal in the manufacturing process of aircrafts. Later, *DuPont* company developed a new composite made of aramide fibre known as Kevlar [20].

Both military and civil aircrafts, boasted a significant ways of possibilities through the application of CFRP and advanced composites.

From the military point of view, both USA and EU started to integrate composites on their fighter planes such as *F-111* and *Eurofighter* until now. Otherwise, on the commercial aviation side, manufacturers used composites on different parts of the aircraft structure [21]. The *Lockheed Tristar* was the first commercial airplane to use Kevlar fibre panels instead of aluminium. Boeing and Airbus also have integrated composites from their beginnings until now. Starting with the Boeing 767 and A-320 Airbus respectively, in which several parts of the wings and floor beams were made of composites, and ending up with the Boeing 787 and the new A-350 XWB, in which more than half of the aircraft's structure is made of composite [3].

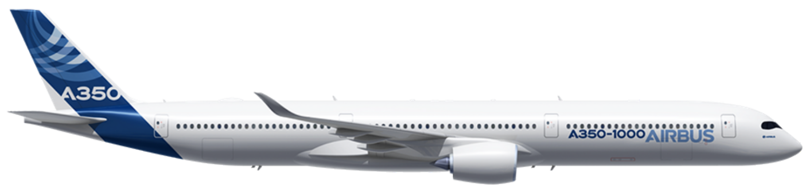


Figure 12: A350-1000 [3]

On the last decades of the last century, impacts on composites was one of the major issues for engineers and researchers, since the damage produced could affect the operating life of the structures and reduced drastically their mechanical and aerodynamic properties [14].

Most of the papers and results were focused on low velocity ballistic impacts and the damages induced into laminate composite materials. However, important aerospace agencies such as NASA studied the behaviour of High Energy Dynamic Impact (HEDI) events to determine the state of the art of this type of high velocity impact in composite fuselage shielding applications. Using computational models as in this project, they were validated against the test data, expanding the background on this field [22]. On the other hand, authors as Abrate on 1994 gathered information about the latest advances and developments [14]. Important results were discovered in terms of the delamination and the ballistic limit. Interface delamination is induced by matrix cracking [17] and its growth induced by matrix bending was confirmed by Choi and Chang in 1992 [23]. Moreover, residual velocity was also studied to determine the energy absorbed during the projectile penetration. In this field Lin and Bhatnagar made an important analysis [24].

In University Carlos III de Madrid, impacts on composites were also studied by J. Pernas [12], G. Castillo [8] and J. Santos [16] who presented their results based on the usage of Finite Element Methods such as Abaqus or LS-Dyna, which will be utilized for this project.

# 3 Methodology

This section will introduce in the first two subsections a detailed description of the experimental test performed in the university from which the experimental data was collected and a brief explanation of the finite element method (FEM) utilized throughout this project which is LS-Dyna®.

Afterwards, all the process to model a composite laminate plate will be explained which encompasses different commands, variables and assumptions which must be taken. The sensitivity of this model will be analyzed comparing it with the experimental data. Therefore, a variation of the size of elements and its correlation with the residual velocity and delamination will be performed. Finally, several impact tests with different variations and boundary conditions will be presented.

## 3.1 Experimental test

In order to make an effective analysis with appropriate models which represent the real behaviour of ballistic impacts, it is necessary to take the real data by performing an experimental test in the University's facilities. As it has been said before, the trials are made with high velocity impacts and to reach that speed a pneumatic canyon is utilized. This equipment works with pressurized light gases such as He or $CO_2$ or compressed air that propels the projectile at the desired velocity, even above 300 m/s.

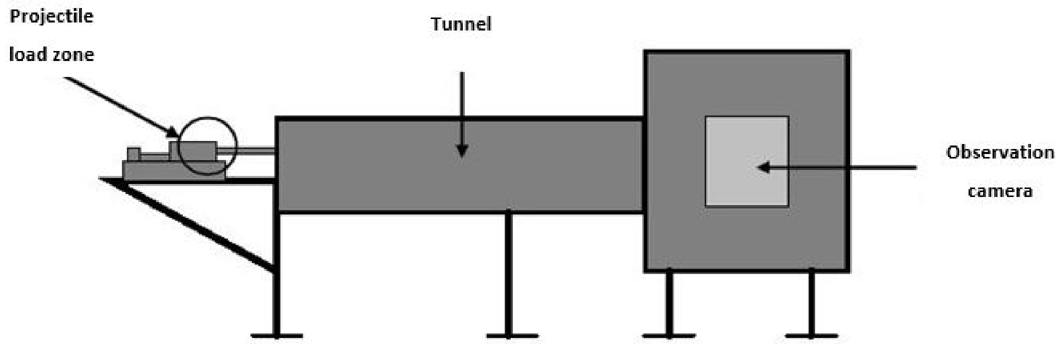


Figure 13: Canyon scheme [8]

A representative illustration of the canyon is detailed in figure 13. The projectile used for the trial is located at the load zone. It has spherical shape with a diameter of 7,5 mm, a mass of 1,73 g and it is made with tempered steel with high hardness [8]. Thanks to these properties, since the trials that are executed are realized with such velocity, plastic deformation on the projectile is avoided. The projectile goes through the 2m long tunnel and reaches the composite panel which is located on the observation chamber and surrounded by sensors that calculates the impact velocity.

The impact is performed perpendicular to the laminate plate. To get that condition, several aluminium C-shaped profiles hold the sample on the edges in the desired position. In this way, the condition of the trial will be clamped.

Referring to the composite, a 110x110 mm$^2$ laminate plate made of 2 laminas is used throughout the trials. The material that composed the panel has a reference of AGP-193-PW which is carbon fibre with epoxy matrix. The thickness of each lamina is similar to the one selected for this project since it is manufactured also by Hexcel® Composites [11]. Therefore the total thickness is around 2.4 mm. The panel is symmnetric with respect to the middle plane and the sequence utilized is (+45/-45/0/90/90/0)s.

Figure 14: Pneumatic canyon pressurized with light gas ($CO_2$ or He) [9]

## 3.2 Introduction to LS-Dyna®

In the past century, automobile, aerospace, manufacturing and engineering industries among others took many time and used expensive supercomputers to test and solve the differential equations behind the dynamics of the impacts in different materials they wanted to analyze. It was a tedious and cumbersome task to accomplish until FEM software made this process easier and more efficient. Specifically, LS-Dyna® is capable of processing highly nonlinear, transient dynamic finite element analysis (FEA) with specific time integration. Therefore, thanks to its nonlinear capability, it will be possible to change the boundary conditions i.e. contact between the projectile and the composite plate, and visualize large deformations since the impact in the composite material used does not exhibit ideally elastic behaviour [25] [26].

As any other finite element method software, LS-Dyna® is capable of solving complex differential equations applied to real world problem simulations. To that aim, it is integrated by LSPrePost® module, which is an advanced pre- and post-processor that applies FEM to discretize the continuous medium by dividing the parts into elements connected by nodes. These divisions will be analyzed and can have different shapes, being tetrahedral and hexahedral the most preferable ones. Apart from that, LSPrePost® also includes the capability to edit, import and export any LS-Dyna® model and provide reports and graphics of the contours, magnitudes and variables given by the numerical solutions [25].

Within this module, the composite laminate plate and the projectile will be design including their material properties. To generate a 3D analysis of the impact in which all the displacements and fractures are visualize with accuracy as in the reality, boundary conditions will be implemented and the type of contact will be also selected.

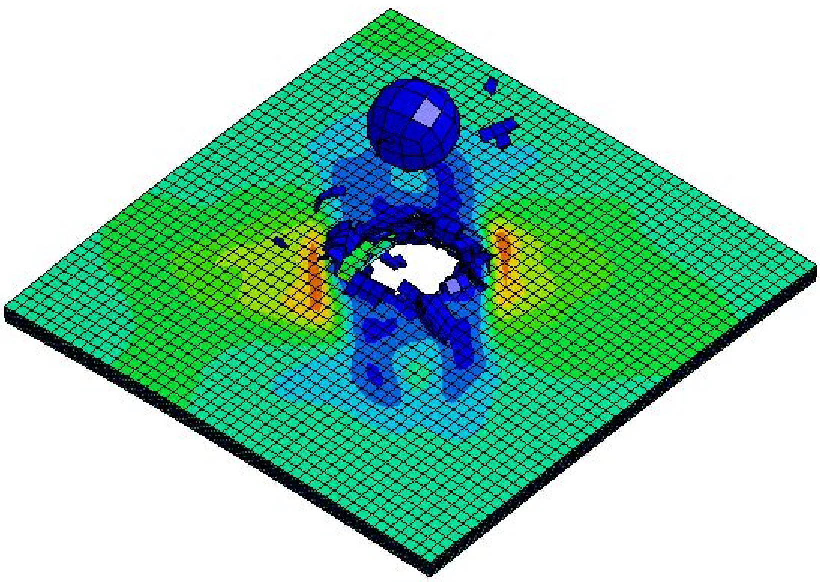

Figure 15: FEM of a ballistic impact by LS-Dyna®

## 3.3 Composite laminate plate modelling

To generate a mesh with the dimensions of the sample plate used in the experimental test explained in *Subsection* 1.3.1, *shape mesher* tool is selected. With this option the coordinates of each lamina that form the plate are entering in x, y and z direction. Moreover, it is possible to assess the number of elements in each ply as well as the geometry of each element, being hexahedral the one selected.

For generating the projectile mesh, the same process is implemented considering its own dimensions (a 7.5mm diameter sphere). To include the properties of the material is made of, tempered steel, *elastic* material model is used and parameters on table 2 are introduced [9].

| $\rho_s$[kg/m$^3$] | E$_s$[$Gpa$] | $\upsilon_s$ |
|---|---|---|
| 7850 | 210 | 0.33 |

Table 2: Projectile material properties

Both type meshes are *solid* since this type provides another dimension in space, instead of the bidimensional or *shell* type one, which is planar. Although the processing cost is greater for the solid type, it offers a more reliable results since the number of nodes and connections between them are much greater than in the shell type (see *Figure* 16) [25]. Besides, the stresses in the perpendicular direction of the plane would have a massive importance in the delamination analysis and the values with this type will be more precise. [16].

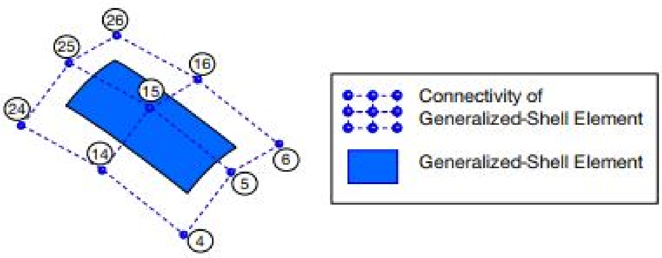


(shell element)

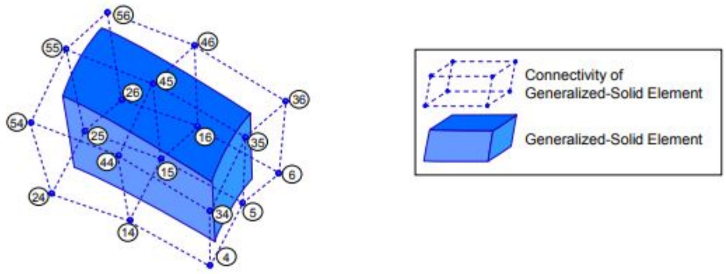


(solid element)

Figure 16: Element types [25]

Including the material properties of the composite plate, shown in table 1, is done by using the material model **Enhanced_composite_damage*. It is also possible include the directions of the fibres in each lamina. Since there are 4 directions of fibres in all the plate (+45,-45,0,90), each lamina will have its own vector of direction for its fibres.

Another important issue is including the Poisson´s ratio in direction 21. This can be easily calculated by taking the mechanical properties given by the manufacturer on table 1 and applying the following equation:

$$\frac{\upsilon_{12}}{E_1} = \frac{\upsilon_{21}}{E_2} \tag{1}$$

which it gives a Poisson´s ratio equals to: $\upsilon_{21} = 0.01996$

**Enhanced_composite_damage* model the material as elastic until the failure appears. To do that, it incorporates the Chang-Chang failure criteria of 1987 [27] in which the failure modes explained in *subsection* 1.3.3 are included. The directions of the stresses involved in those equations are represented in figure 17.

- **Fibre breakage:**

$$e_f^2 = \left(\frac{\sigma_{11}}{\chi_t}\right)^2 + \left(\frac{\sigma_{12}}{S_{12}}\right)^2 \tag{2}$$

- **Matrix cracking under traction (3) and compression (4):**

$$e_m^2 = \left(\frac{\sigma_{22}}{\Upsilon_t}\right)^2 + \left(\frac{\sigma_{12}}{S_{12}}\right)^2 \Leftrightarrow \sigma_{22} > 0 \tag{3}$$

$$e_m^2 = \frac{1}{4}\left(\frac{-\sigma_{22}}{S_{12}}\right)^2 + \frac{\Upsilon_c \sigma_{22}}{4S_{12}^2} - \frac{\sigma_{22}}{\Upsilon_c} + \left(\frac{\sigma_{12}}{S_{12}}\right)^2 \Leftrightarrow \sigma_{22} < 0 \tag{4}$$

- **Delamination:**

$$e_l^2 = \left(\frac{\sigma_{33}}{Z_t}\right)^2 + \left(\frac{\sigma_{23}}{S_{23}}\right)^2 + \left(\frac{\sigma_{13}}{S_{13}}\right)^2 \tag{5}$$

Being $e_i$ the determination of the failure. Thus, $e_i = 0$ means "no failure" and $e_i = 1$ means "completely failure".

Finally, in order to make an effective simulation of the delamination failure, it is needed to model a cohesive interaction between the laminas of the plate. This will increase the computational cost of the process but the prediction of the damage will be more accurate, specially for the delamination. This will be made by using the option **Contact_automatic_surface_ to_surface_tiebreak* in which solid elements will be ruled by a Discrete Crack Model [25].

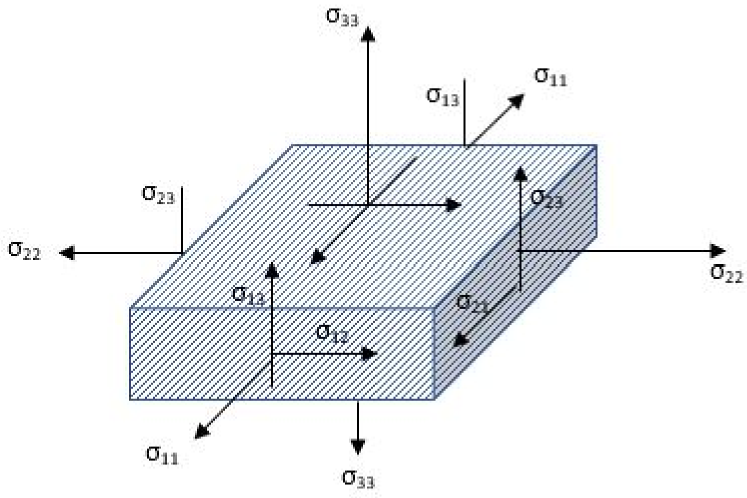


Figure 17: Representation of the stresses involved and their directions

Before implementing this new modeling feature, it is necessary to define several parameters in normal and tangential direction to the plane, which are summarized in table 3:

| Parameter | Value |
|---|---|
| T [MPa] | 40 |
| $S$ [MPa] | 65 |
| $G_I$ [J/m] | 250 |
| $G_{II}$ [J/m] | 750 |

Table 3: Parameters for the cohesive interaction model

In this cohesive material model, the ultimate displacements in normal and tangential direction follow a bilinear traction-separation law in which previous parameters are involved.

$$G_I = \frac{1}{2} T u_n \tag{6}$$

$$G_{II} = \frac{1}{2} S u_t \tag{7}$$

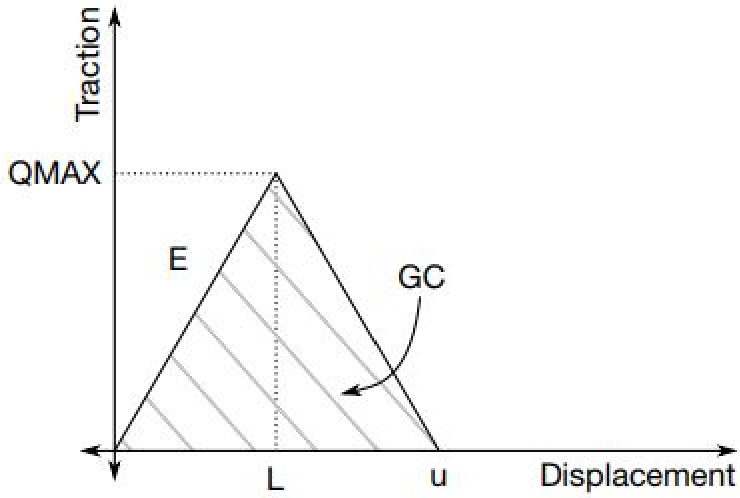


Figure 18: Bilinear traction-separation law [26]

Alternatively, the total relative displacement $\delta_m$ given by $\delta_m = \sqrt{\delta_I^2 + \delta_{II}^2}$, is governed by a mixed-mode criterium since it encompasses the separation in normal and tangential direction ($\delta_I$ - mode I and $\delta_{II}$ - mode II) respectively.

As any failure mechanism, the mixed-mode displacement is formed by an initiation and propagation law. Thus, the damage initiation displacement $\delta^0$ is given by equation 8.

$$\delta^0 = \delta_I^0 \delta_{II}^0 \sqrt{\frac{1+\beta^2}{(\delta_{II}^0)^2 + (\beta\delta_I^0)^2}} \tag{8}$$

where $\delta_I^0 = \mathrm{T}/\ \mathrm{kN}$ and $\delta_{II}^0 = \mathrm{S}/\ \mathrm{kT}$ are the single mode damage initiation separations with kN and kT the respective stiffness of the cohesive element, and $\beta$ is called the "mode mixity".

The ultimate mixed-mode displacement $\delta^F$ (total failure) can be modelled by either a power law or the B-K damage model. For this project the second one was implemented and it provides the following equation:

$$\delta^F = \frac{2}{\delta^0 \left( \frac{1}{1+\beta^2} k_N^\gamma + \frac{\beta^2}{1+\beta^2} k_T^\gamma \right)^{\frac{1}{\gamma}}} \left[ G_I + (G_{II} - G_I) \left( \frac{\beta^2 k_T}{k_N + \beta^2 k_T} \right)^{|\alpha|} \right] \tag{9}$$

For the sake of completeness, figures 18 and 19 illustrates the mixed-mode damage mechanism by delamination in which it is possible to know and visualize what represents each of the parameters included in previous equations.

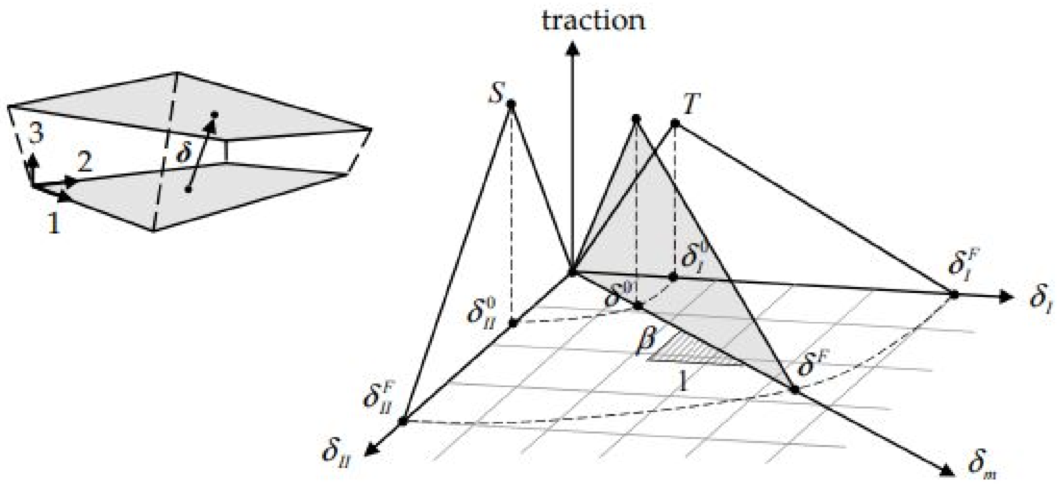


Figure 19: Mixed-mode traction-separation law for the cohesive element [26]

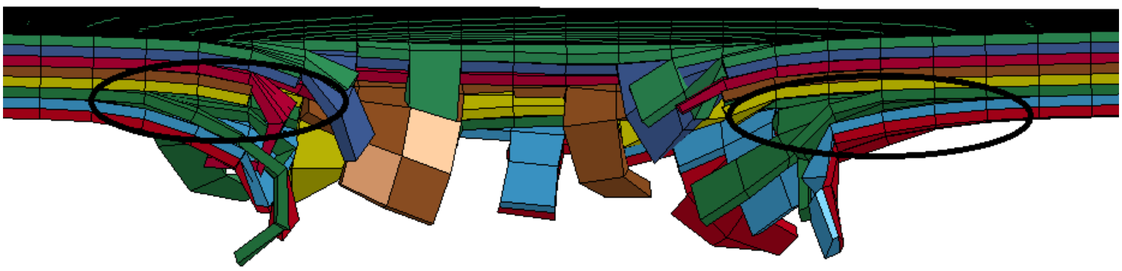

Figure 20: Delamination simulation by LS-Dyna®

## 3.4 Validation

Before starting with the ballistic tests, it is necessary to select the correct meshes for the plate and the projectile. By doing this sensitivity analysis, previous formulations and mechanics that exist behind the generated meshes will be evaluated and compared with the results of the experimental case in terms of residual velocity and delaminated area . If the similarity is evident, those meshes will be the ones used onwards on this project for the different cases to be analyzed.

Moreover, this preliminary analysis will confirm whether the simulation of the entire model is correct and completely realistic. All the criteria and equations included on the program, the material and cohesive modelling, the contact between the surfaces once the impact is produced and the boundary conditions applied will be also assessed.

This selection process is based on the number of hexahedral solid elements in which the meshes are going to be divided. The more number of elements for a mesh, the larger will be the processing cost but this does not imply the larger similarity with the experimental case. In the case of the plate, 8 laminas are stacked. Each one has the dimensions specified in *subsection* 1.3.1 but 3 different divisions of elements are performed: 1 division per 1 mm, 1 division per 2 mm and 1 division per 3 mm.

| | div/mm | Elements/Lamina | Total elements |
|---|---|---|---|
| Mesh 1 | 1/3 | 36x36 | 10752 |
| Mesh 2 | 1/2 | 55x55 | 24200 |
| Mesh 3 | 1/1 | 110x110 | 96800 |

Table 4: Divisions of the laminate plate meshes analysed

To generate the results it is necessary another mesh for the projectile. Since this mesh will be analyzed later on, once the plate mesh divisions are selected, a standard sphere with 1000 elements is created.

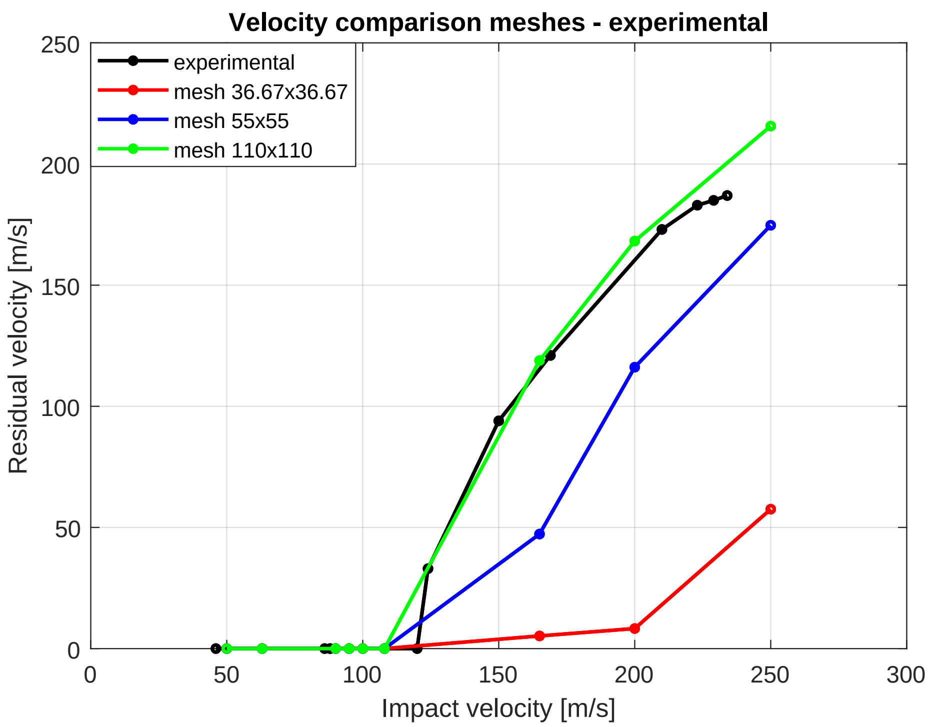


Figure 21: Comparison of residual velocities between the computational meshes and the experimental case

In figure 21 it can be seen the velocity results of the different plate meshes analyzed and compared with the experimental data (black). An important aspect of this first plot is the zero values found in all the cases. The reason is that until the projectile gets a high enough velocity to go through the plate, the sphere bounces on the plate surface displaying positive values or get embedded on the laminas with negligible speed. Once the ballistic limit is reached and the sphere goes through the plate, the residual velocity is registered and increases as the impact velocity does. For the sake of simplicity, if the projectile cannot go through, the velocity value displayed is 0.

As it is seen, the mesh with the lowest number of element divisions (mesh 36x36 - red) gets a poor similarity with respect the others two cases. Even with high impact velocity, the projectile does not go through the plate with a significant residual velocity. The remaining cases, both the mesh 55x55-blue and mesh 110x110-green, display an expected behaviour very consistent. Specially, the mesh with the rate of 1/1 div/mm (110x110) represents the same behaviour as the experimental data.

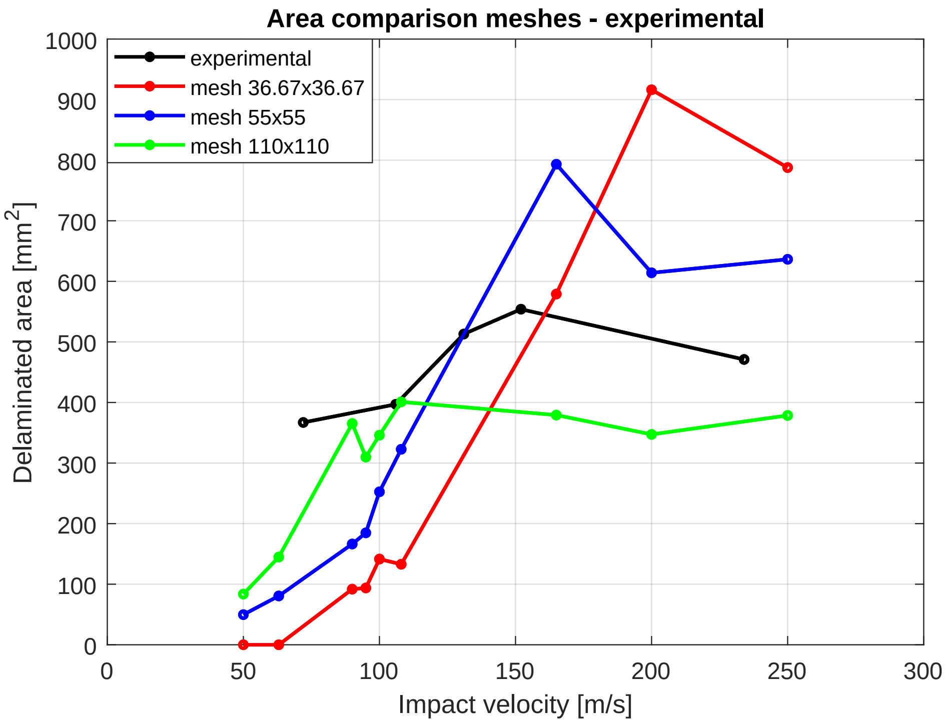


Figure 22: Comparison of delaminated area between the computational meshes and the experimental case

After the velocity results, the delaminated area is plotted (figure 22) for the different meshes. Unlike the previous graph, in this case there is no zero values. Even if the ballistic limit is not reached (no penetration is produced), delamination starts to appear inside the plate. As it is observed with the experimental data (black), once the penetration is produced, the area delaminated increases as the impact velocity does. It is true that this behaviour is represented on mesh 36x36-red and 55x55-blue but in a very abrupt way. However, although the similarity between the 110x110 case (green) and the experimental one is lower than previous graph, this mesh displays the delamination more consistent than previous two types of meshes.

| | Residual velocity [m/s] | | | |
|---|---|---|---|---|
| Impact velocity [m/s] | experimental | 36x36 | 55x55 | 110x110 |
| 124 | 33 | 2 | 18 | 50 |
| 150 | 94 | 5 | 32 | 94 |
| 169 | 121 | 5.22 | 48 | 120 |
| 210 | 173 | 12 | 128 | 176 |
| 234 | 187 | 40 | 155 | 200 |
| Average deviation | | 91.2% | 76.2% | 12.2% |

Table 5: Values of residual velocities and deviations for the cases analysed

Making a more exhaustive analysis of the velocity results based on the deviation of the meshes with respect to the real data, the 110x110 case is the best configuration of mesh division with 1 div/mm. This selection is completely approved because its deviation with respect to the real case is about 12.2% as it appears on table 5.

| | Delaminated area [$mm^2$] | | | |
|---|---|---|---|---|
| Impact velocity [m/s] | experimental | 36x36 | 55x55 | 110x110 |
| 72 | 367 | 40 | 100 | 200 |
| 90 | 366 | 91.8 | 166 | 365.2 |
| 106 | 397 | 130 | 320 | 397 |
| 131 | 513 | 300 | 513 | 399 |
| 152 | 554 | 460 | 680 | 390 |
| 200 | 500 | 910 | 610 | 355 |
| 234 | 471 | 820 | 622 | 360 |
| 250 | 452 | 787 | 636 | 379 |
| Average deviation | | 65% | 33% | 20.7% |

Table 6: Values of delaminated area and deviations for the cases analyzed

On the other hand, making the same analysis with the area delaminated in table 6, the selection of 110x110 plate mesh is well justified with a low value in deviation with respect to the real data (20.7%).

With that laminate plate mesh, it is time for determining the projectile mesh. Since previous analysis were made with a sphere of 1000 elements, a range in which 1000 elements were included was agreed, to study the correlation of the results increasing the number of sphere elements progressively.

| Sphere | Element Density | Total Elements |
|---|---|---|
| Sphere 1 | 3 | 190 |
| Sphere 2 | 4 | 448 |
| Sphere 3 | 5 | 875 |
| Sphere 4 | 6 | 1512 |

Table 7: Sphere types considered

Element density parameter that appears on table 7 is related with the number of layers that surrounds the nucleus of the solid sphere. For the sake of clarity, figure 23 shows each of the cross section of the sphere meshes.

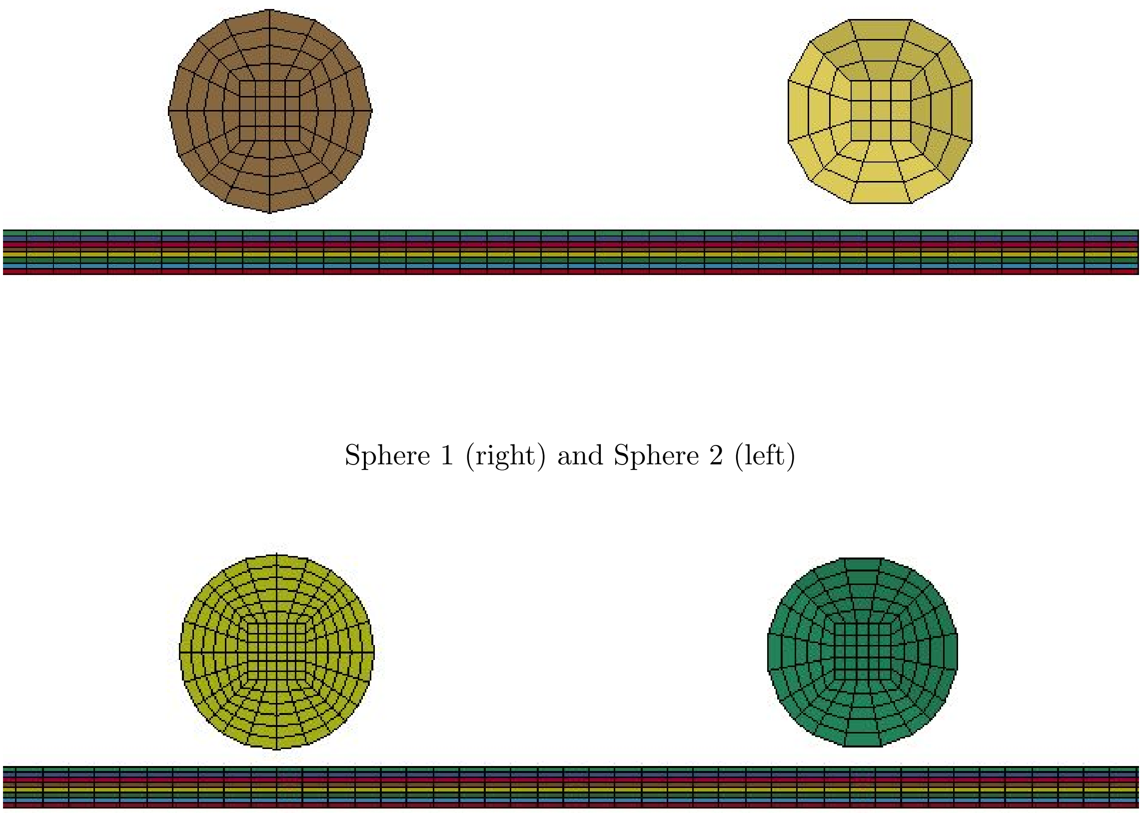

Sphere 1 (right) and Sphere 2 (left)

Sphere 3 (right) and Sphere 4 (left)

Figure 23: Cross sections of the projectiles

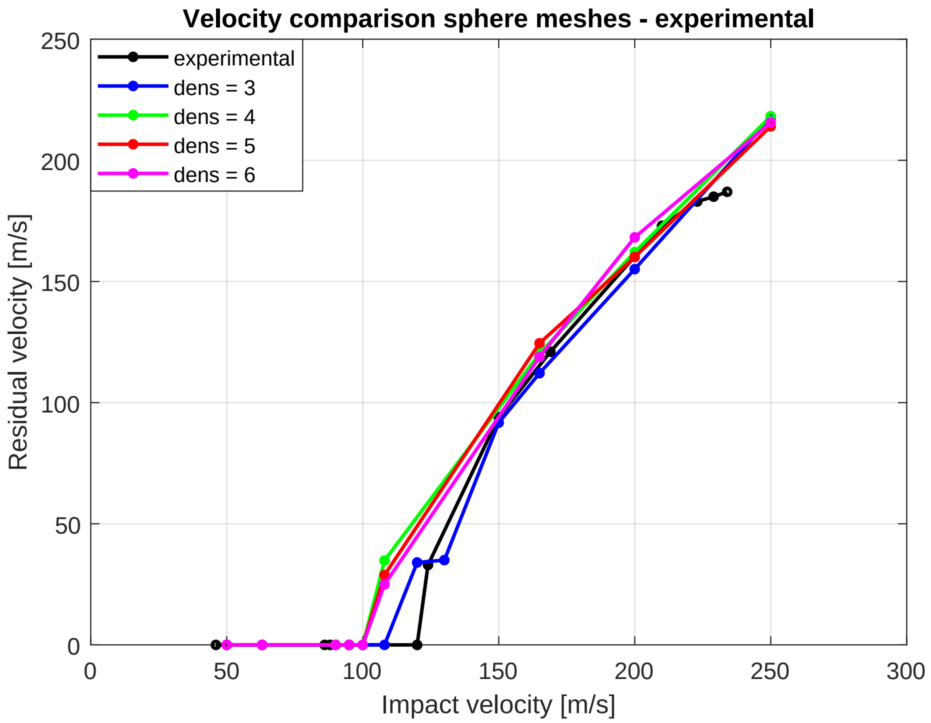


Figure 24: Comparison of delaminated area between the sphere meshes and the experimental case

Previous comments about the behaviour, interpretation and tendency of the plate meshes analyzed are also valid for this analysis with the sphere meshes.

Based on results shown in figures 24 and 25 in terms of residual velocity and delaminated area, any of both sphere 1 (dens=3) or 4 (dens=6) is valid to continue with the analysis. However, sphere 1 (dens=3) is selected as the definitive projectile mesh because it presents a slightly better similarity with the real case than sphere 4 (dens=6) and since the laminate plate has already a considerable number of nodes and elements, the total processing cost of the whole analysis will be lower than selecting sphere 4 with a greater density which provides more elements.

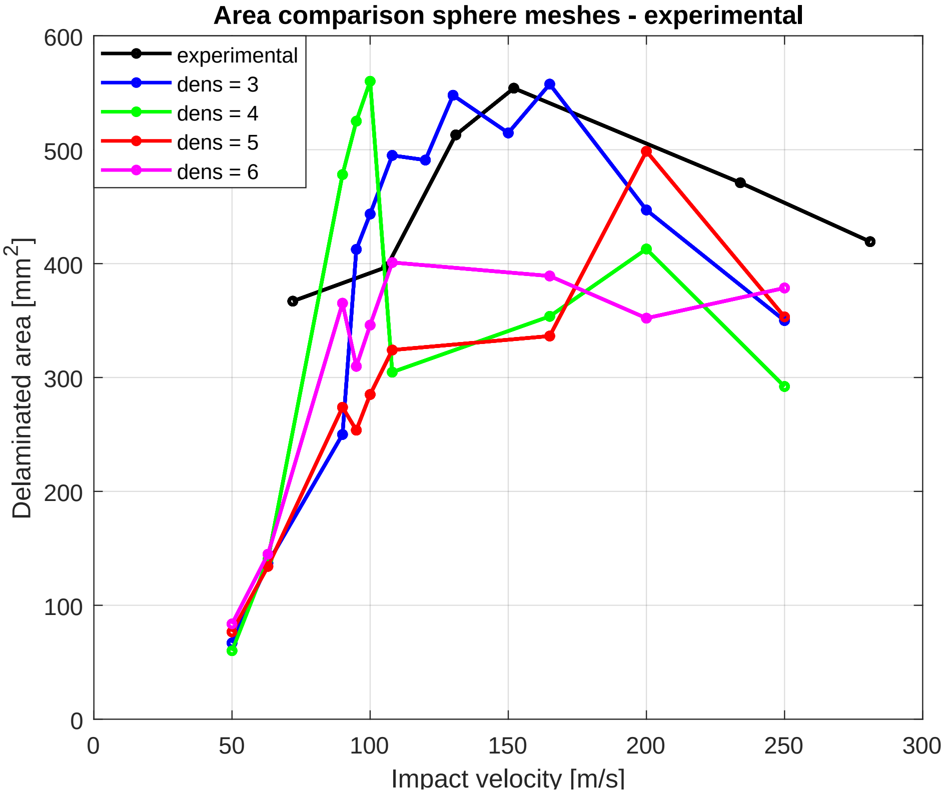


Figure 25: Comparison of residual velocities between the sphere meshes and the experimental case

After the realization of these comparisons between different plate and sphere meshes, the conclusion is the following:

From this point onwards, the base case in which the required variations are going to be performed, is going to be composed of two parts: a laminate plate mesh with 1 div/elem giving a total of 110x110 elements in each lamina and a projectile mesh with spherical shape and 190 elements which means a density=3.

A simple view of the selected cases is represented below in figures 26 and 27 representing the results in residual velocity and delaminated area where it is perfectly seen how the model represents in a consistent and accurate way the reality.

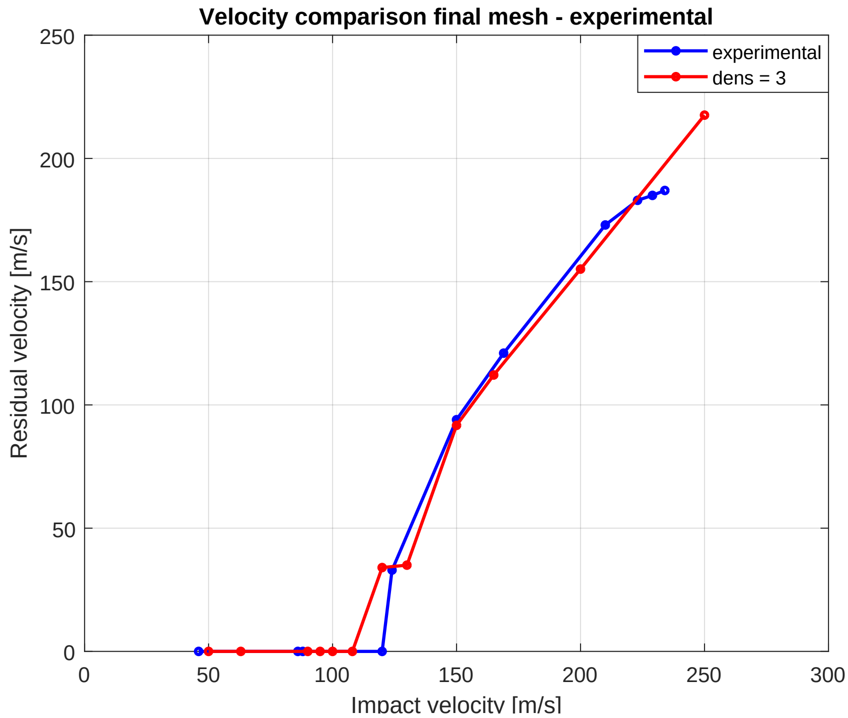


Figure 26: Final residual velocity results

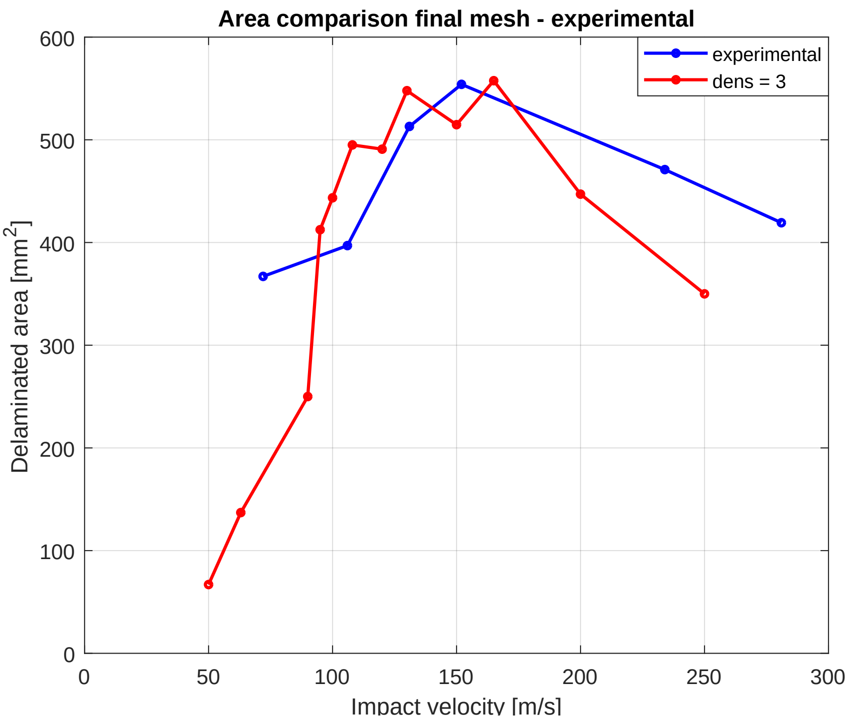


Figure 27: Final delaminated area results

As a final step, to confirm the validation of the interlaminar failure model with which previous graphs have been produced, the cohesive set of elements between the plies is inspected.

In the real case, when the projectile penetrates on the plate, plies start to delaminate and separate from each other following the direction of the fibres are composed of. In the case of two adjacent laminas made of fibres at 45º and -45º respectively, the delamination pattern will follow both directions. Effectively, the model verifies this statement in figures 28 and 29 where the shape that the projectile leaves once it goes through the plate is seen easily.

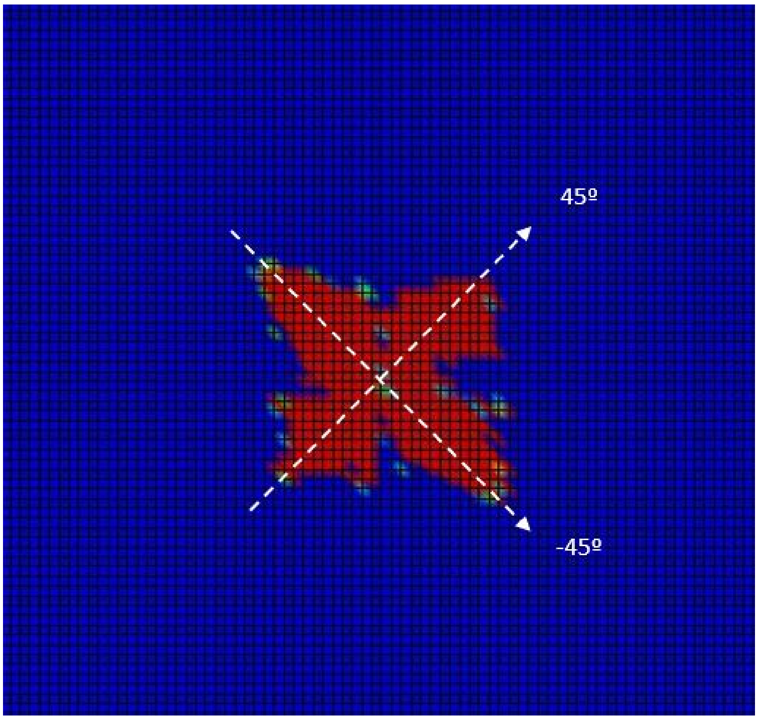


Figure 28: Delamination pattern of the cohesive element between laminas at 45º and -45º respectively

As it was explained before in this section, equations 2, 3, 4, and 5 determined the failure depending on the value of the solution: 1 is damaged, 0 is elastic (not damaged).

In the same way, to display the images of the delamination, the model represents the whole plate and distinguish if the plate is damaged or not depending on the color is shown. For this case, if there is no damage in a certain region the model print that part in blue ( value = 0 ). Otherwise, the part is colored in red ( value = 1 ).

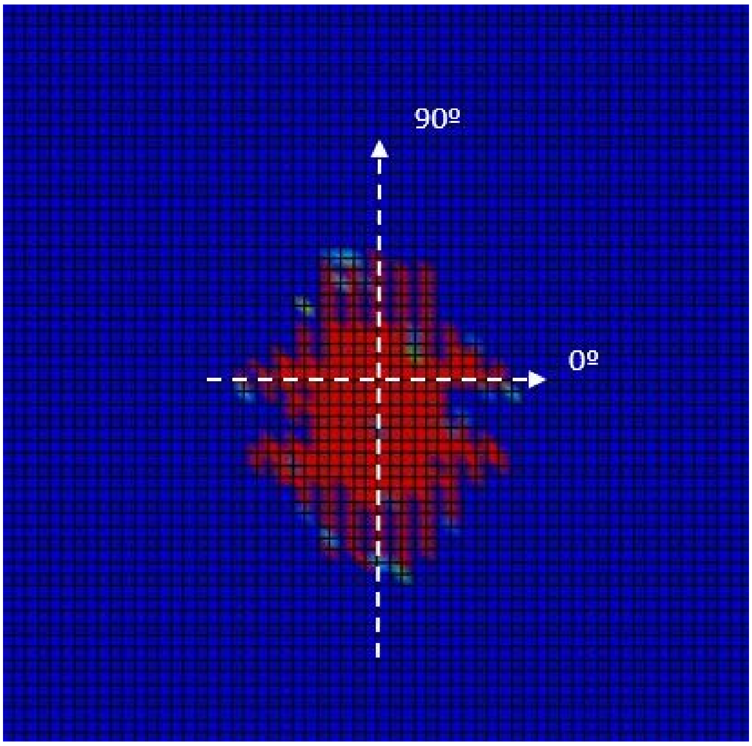


Figure 29: Delamination pattern of the cohesive element between laminas at 0º and 90º respectively

## 3.5 Cases subjected to analysis

After the sensitivity analysis in which both projectile and laminate plate meshes have been determined, the following cases are going to be studied:

- Variation of the laminate plate dimensions
- Variation of the laminate plate thickness
- Variation of the laminate plate boundary conditions
- Variation of the laminate plate mechanical properties

### 3.5.1 Variation of the laminate plate dimensions

Within this section two types of variations are distinguished making the plate quadrangular and rectangular:

1. Quadrangular shape

   In this case, two different plates of 50x50 mm and 165x165 mm will be compared with the 110x110 mm one, taking into account the area that is delaminated by the impact and the residual velocity of the projectile.

2. Rectangular shape

   As in previous case, results based on delamination and residual velocity of the original plate will be studied with the ones obtained from a 55x110 mm plate and a 165x110 mm plate.

After these cases, it will be determined if there exist any influence on delamination and residual velocity due to a variation in the geometry of the composite laminate plate.

### 3.5.2 Variation of the laminate plate thickness

The original composite plate is composed of 8 plies of laminas. As it was explained on *subsection* 1.3.1 and figure 6, its stacking sequence is $(+45^{\circ}/-45^{\circ}/0^{\circ}/90^{\circ})_s$. In this section, the thickness of the composite plate is augmented. This is done precisely by increasing the number of laminas up to 12, so the total thickness of the new plate analysed is 2.4 mm. Moreover, the stacking sequence is changed with the final configuration of $(+45^{\circ}/-45^{\circ}/0^{\circ}/90^{\circ}/90^{\circ}/0^{\circ})_s$ as it can be seen in figure 30.

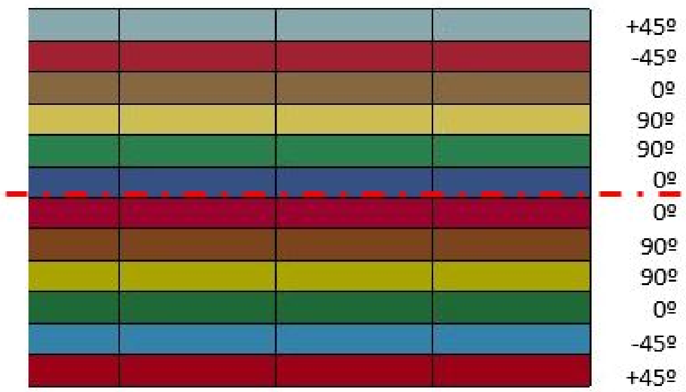


Figure 30: Stacking sequence of the 12-lamina plate

After the analysis, it will be determined the variation in delamination and residual velocity that provokes the variation in thickness.

### 3.5.3 Variation of the laminate boundary conditions

Up to this point all the cases subjected to be analysed are simply supported at all the edges of the plate. In this section this boundary condition will be changed, maintaining the same plate geometry (110x110mm), by:

- Simply supported at the bottom lamina edges
- Clamped at the bottom lamina edges
- Clamped at all edges
- Free at all edges

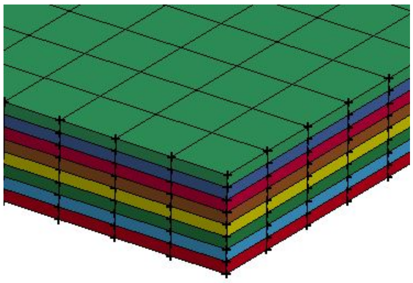

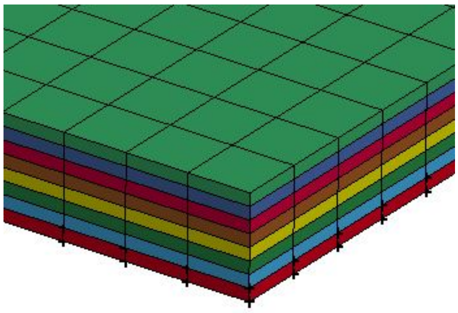

Figure 31: Zoom in at all nodes clamped (left) and at the bottom lamina nodes clamped (right)

With this analysis, it will be determined if there exists any correlation between the different boundary conditions applied and the results of interlaminar failure and residual velocity.

### 3.5.4 Variation of the laminate plate mechanical properties

The last variation to be studied will be changing the mechanical properties of the material. Specifically, some of the principal properties appearing on table 1 such as the fibre density, the longitudinal compressive and tensile strengths, the transverse compressive and tensile strengths and the shear strength. All these parameters are multiply by a factor of 1,5. On the other hand, it will be changed also the properties of the cohesive model shown in table 3. Normal and shear stresses, shear energy release rate and normal stiffness will be multiply also by the same factor as before.

These changes will determine which properties affect more to the delamination and residual velocity. The new values of the parameters are displayed on table 8.

| Mechanical properties | | | | |
|---|---|---|---|---|
| $\chi_c[Mpa]$ | $\chi_t[Mpa]$ | $\Upsilon_c[Mpa]$ | $\Upsilon_t[Mpa]$ | **S** [Mpa] |
| 2484 | 3157 | 262.5 | 118.5 | 171 |
| Cohesive properties | | | | |
| **T** [Mpa] | ***S*** [Mpa] | $\mathbf{G}_{II}$ [J/m] | CN | $\rho$f [kg/m$^3$] |
| 60 | 96 | 1125 | 60000 | 2370 |

Table 8: New property values

# 4 Results and discussions

In this section, results in terms of the interlaminar failure and residual velocity of the projectile will be presented. In order to make a realistic analysis, they will be compared to the model case determined in *subsection* 3.3. For maintaining the order throughout this part, they will be divided according to the variation implemented on the model.

## 4.1 Effect of dimensional variation

There will be a distinction between the results of variation in quadrangular shape and the ones of variation in rectangular shape:

- Quadrangular shape

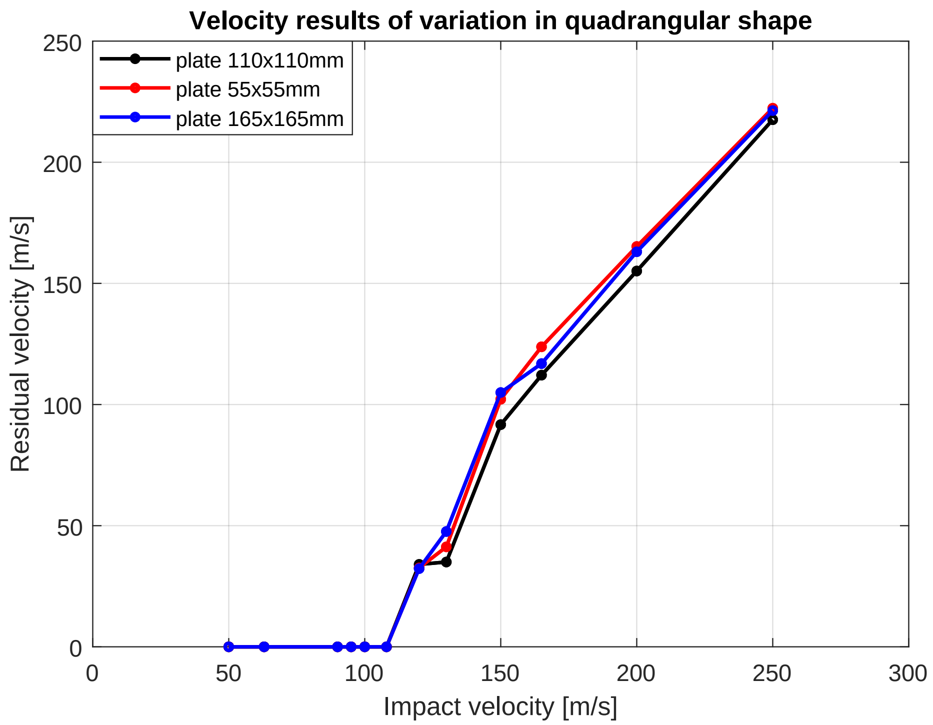


Figure 32: Comparison of delaminated area between the original case and the quadrangular variations

In figure 32, residual velocity results of the three cases present a very high similarity. Plate 165x165 (blue) starts to penetrate a bit earlier than the 110x110 plate (black) and 55x55 plate (red). However, as the impact velocity increases, the tendency turns around but at the end, the difference between the original case and the two variations is very small and it may be due to the errors associated with the large number of elements analyzed in the compilation process.

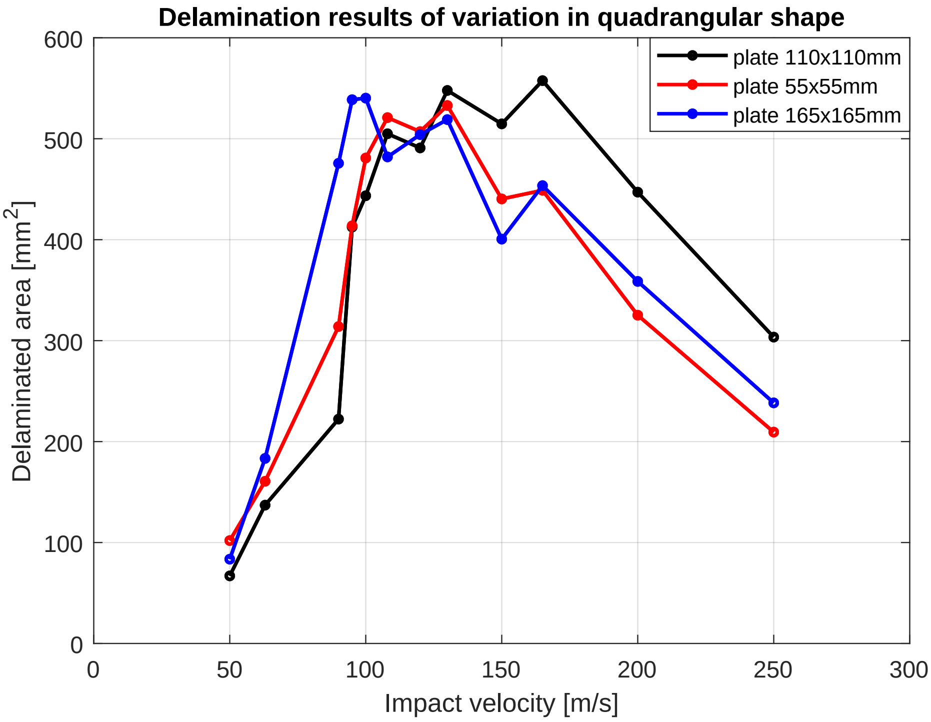


Figure 33: Comparison of residual velocities between the original case and the quadrangular variations

As it can be seen in figure above, interlaminar results of laminate plates 55x55mm and 165x165mm are pretty similar with the ones of the original case 110x110mm. This similarity is verified in those velocity values around the ballistic limit [100 m/s-130 m/s]. Although the tendencies separates each other as the velocity increases from previous range, they share the same behaviour because the area decreases progressively after a slight peak.

This may be explained by fluctuations between laminas in which the deleted elements as the projectile goes through the plate, take part in the compilation process.

- Rectangular shape

In this case, the residual velocity plotted in figure 34 is pretty similar in the three cases as it happens before. However, it is seen that plate 55x110mm (red) penetrates a bit earlier than other two cases, and this tendency is maintained as the velocity increases. This may be explained due to the difference in longitude between the plates. Since the stresses are different in the 2 axis of the plane, this provoke that this plate breaks earlier than the remaining ones and eases the penetration. The 165x110mm plate (blue) recoveries that initial gap and ends up having the same value than the 55x110 mm plate. Globally, same behaviour is observed and there is not too much difference with respect to the original case 110x110mm (black).

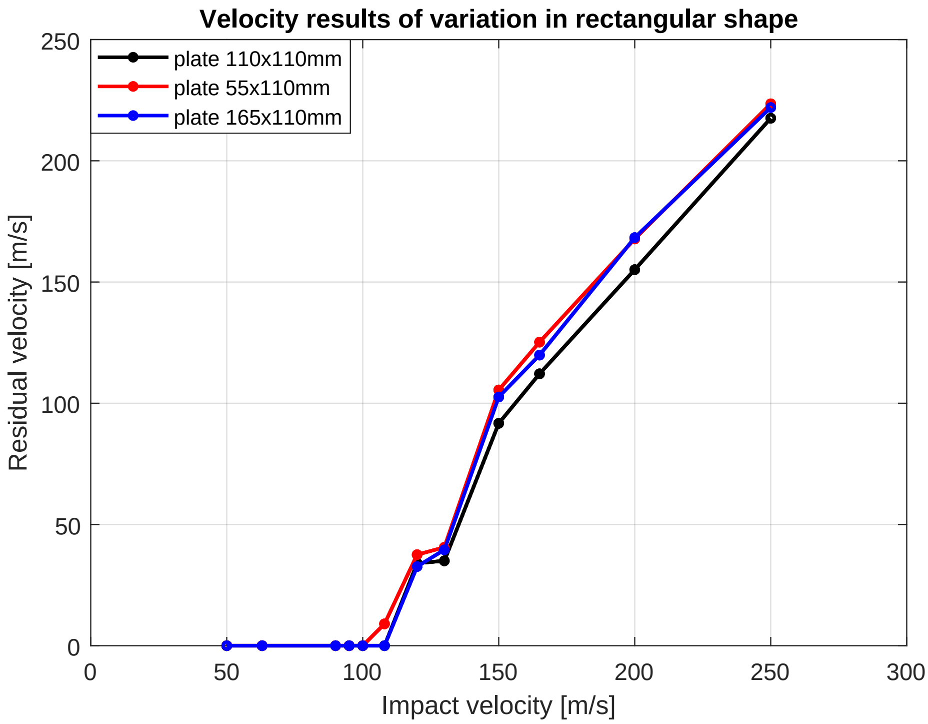


Figure 34: Comparison of delaminated area between the original case and the rectangular variations

However, delamination results in figure 35 show a greater difference than the ones presented in the previous variation type. A possible reason of this change is the geometry utilized with respect to the previous cases. This time, there not exist the same number of element in x and y direction and this may influence the result of the delaminated area. Moreover the explanation given in the quadrangular case is also valid although the behaviour is also maintained.

To sump up this little section of results, dimensional variations do not affect too much to the velocity results. Practically, the same behaviour is present in all the cases and the difference is not significant at all. On the other hand, although the area results show bigger differences, they do not present an extraordinary or noticeable tendency. For this reason, in future ballistic analysis, little samples can be tested instead of large ones in order to save money and material. Moreover, high velocity impacts provides locally effects and initial conditions like these ones do not have a big influence as it has seen in this section and it will be seen afterwards on the project.

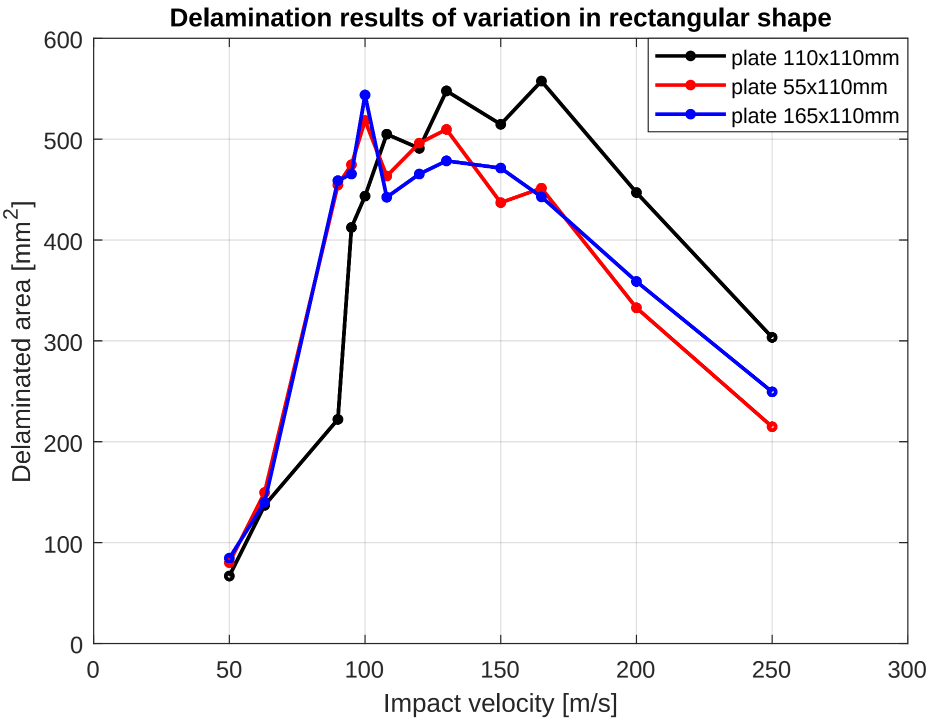


Figure 35: Comparison of residual velocities between the original case and the rectangular variations

## 4.2 Effect of thickness variation

In this section, velocity results on figure 36 reflects what it was expected in advanced. The thicker the plate is, the more difficult is to go through it, so the velocity values of the 12-lamina plate (red) are lower than the thinner one. For this reason, the most important effect of adding more laminas is the delay of the penetration into the material, so the ballistic limit is shifted towards the right hand side of the graph.

Delamination results show a clear difference between the plates as thickness increases. As it can be observed in figure 37, the more laminas the composite plate is composed of, the more delaminated area is generated after the impact. Moreover, it is proved, as it was explain by Abrate, that as the impactor gets more kinetic energy, (gets more velocity in this case) the delaminated area increases [14], as it is plotted on the right hand side of the graph. Comparing the results of both cases, it is widely remarkable that increasing the thickness reduces considerably the failure by delamination before the ballistic limit is reached. Nevertheless, this case also reflects the same behaviour in both plates as previous cases. When the projectile gets enough velocity to go through the plate, the area decreases since the plate breaks easier.

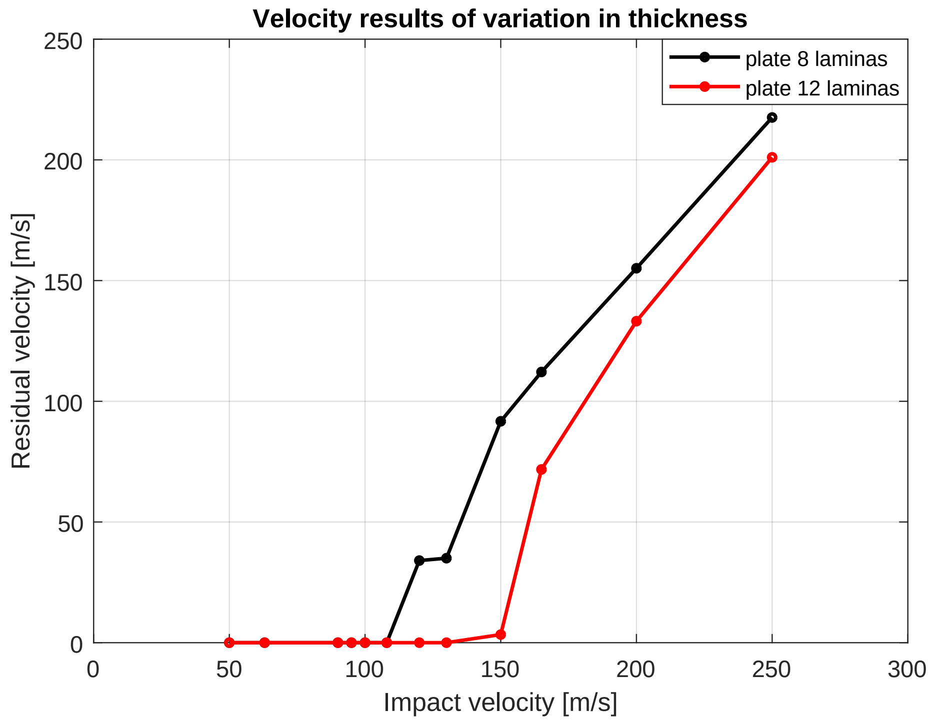


Figure 36: Comparison of delaminated area between plates with different thickness

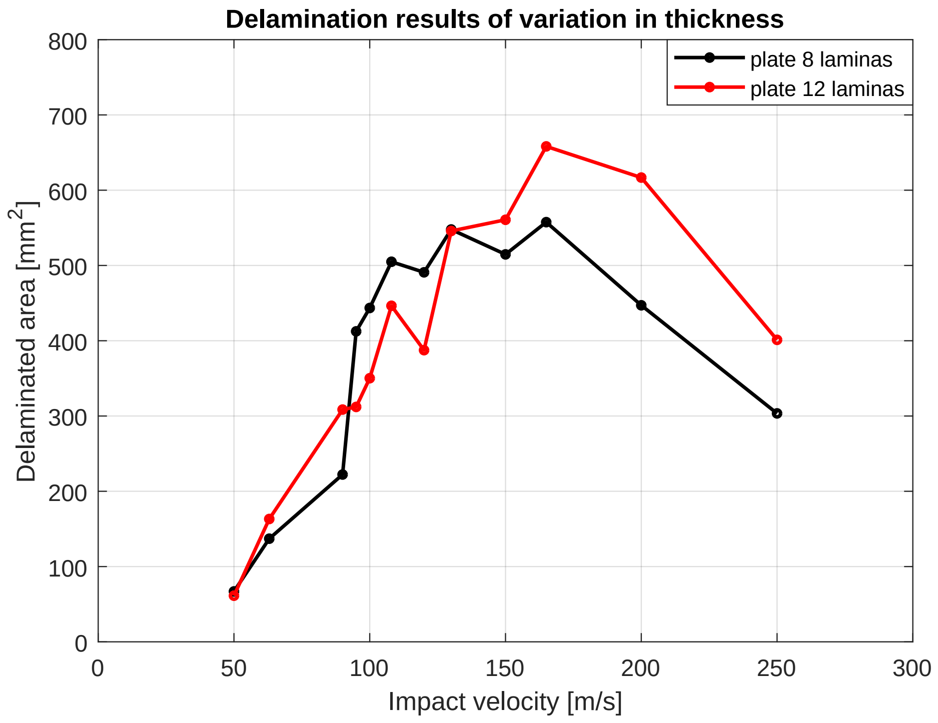


Figure 37: Comparison of residual velocities between plates with different thickness

As a brief discussion, in order to improve the penetration and avoid as much as possible the failure of the plate induced by delamination, adding more and more laminas is crucial and will stop this phenomenon.

## 4.3 Effect of boundary condition variation

It has been discussed previously the influence of changing the geometry and thickness of the laminate plate but always under the same condition: simply supported at all edges. This time, figures 38 and 39 plot the five types of boundary conditions analyzed.

Residual velocity values of the plates with different boundary conditions show a noteworthy behaviour since the similarity is about 100% (see figure 38).This means that whatever the boundary condition applied at the plate edges, it is not relevant to the residual velocity since the response is the same in any case.

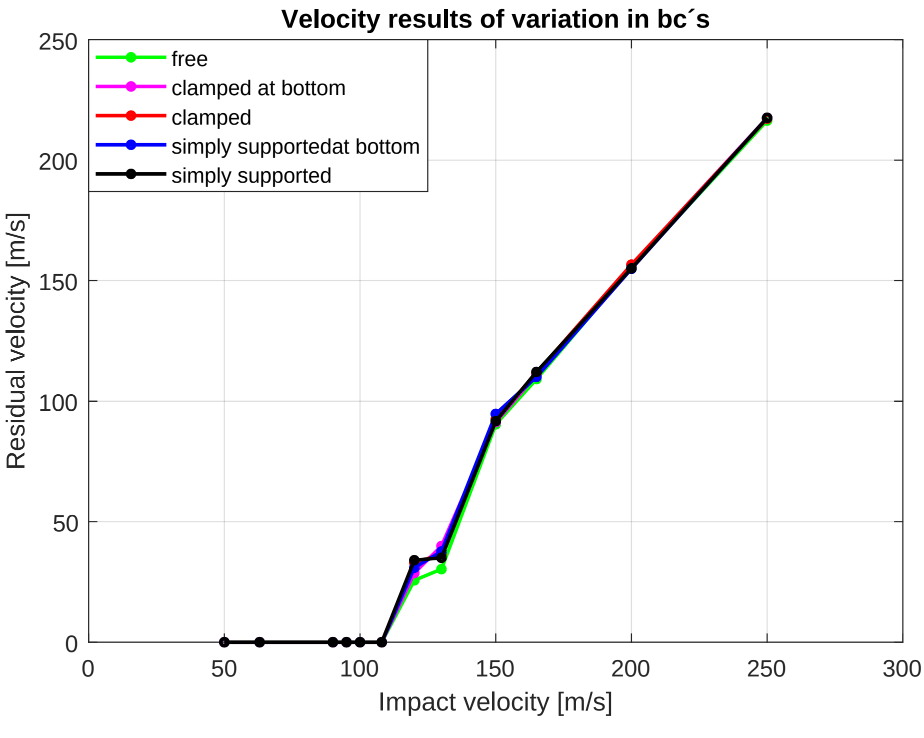


Figure 38: Comparison of delaminated area between plates with different bc´s

It is also remarkable that roughly the same values of area are registered for the same type of condition (figure 39), i.e., fully simply supported (black) and simply supported at the bottom lamina edges (blue) show the same behaviour and the same delaminated area at each testing point. The same applies to fully clamped at all edges (red) and just at the bottom lamina edges (pink).

Laminate plate with free condition (green) is the one that represent the more delamination. It is neither fixed nor supported at any edge of the laminas. This condition may create a plate more flexible or otherwise, it is not able to withstand the same way as other cases did before. The plate is at the expense of the impact velocity and this may produce more damages.

Nevertheless, it is noticeable that in spite of having different values, the difference between them is not so large, at high velocity impacts the effect is very locally so this type of variation does not mean a big issue.

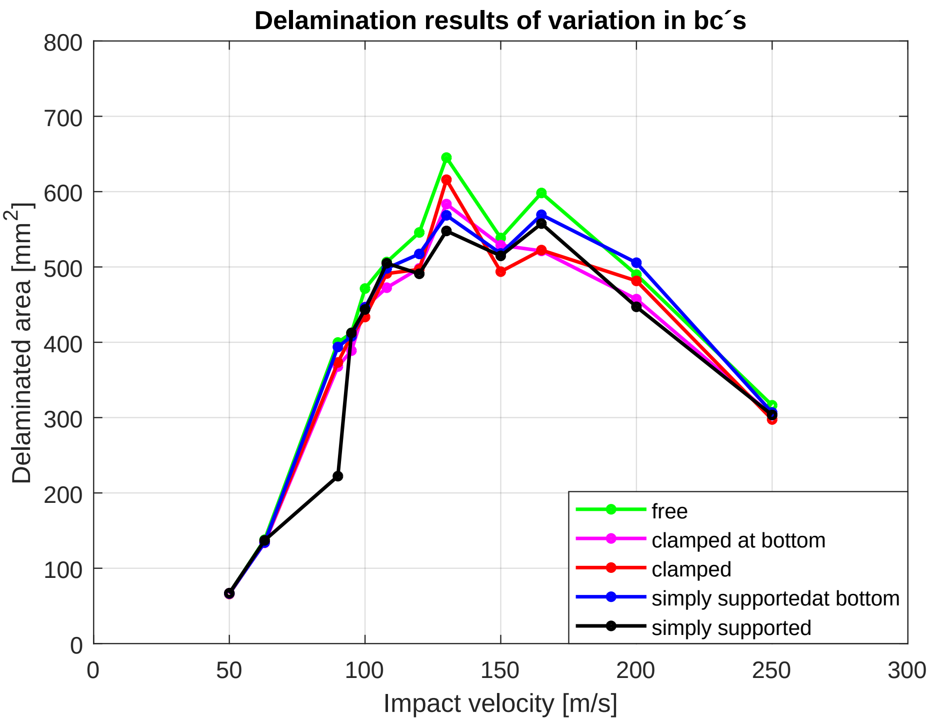


Figure 39: Comparison of residual velocities between plates with different bc´s

On this type of analysis and ballistic impacts, boundary conditions are sometimes very difficult to estimate. However, with these results, it is noticeable that they do not affect too much to the results considered in this project: delamination and residual velocity.

For this reason, refering to real cases, it is true that aircraft boundary conditions will be different than the ones present in this paper but following the conclusion extracted in this part, they do not have a big influence. Moreover, this conclusion is fully consistent with previous reasoning, if the geometry does not have any important influence, the boundary conditions neither should do.

## 4.4 Effect of material property variation

Velocity results of variation in longitudinal/transverse compressive/tensile strengths are shown in figure 40. This time only velocity testing points around the ballistic limit are analyzed since it would be the important range to be discussed.

As it is seen, no big differences in behaviour are plotted. However, it is remarkable that for longitudinal strengths, the variation in compressive one (red) starts to penetrate earlier than the tensile one (blue). These two properties are related to the fibres of the material. Stresses created by the impact affect more to the fibres in the perpendicular direction of the plane than in the parallel one, because provoke their breakage. However, the fibres withstand better those stresses parallel to the direction in which they are oriented to, therefore the tensile strength (blue) delays the ballistic limit with respect to the compressive one. On the other hand, for transverse strengths, the behaviour is the opposite one, tensile strength variation (pink) breaks earlier than the compressive one (green), so the ballistic limit is shifted towards the left. The reason would be the opposite one with respect to the fibres. This time stresses parallel to the plane makes the rupture of the matrix creating more cracks and flaws than those stresses perpendicular to the plane.

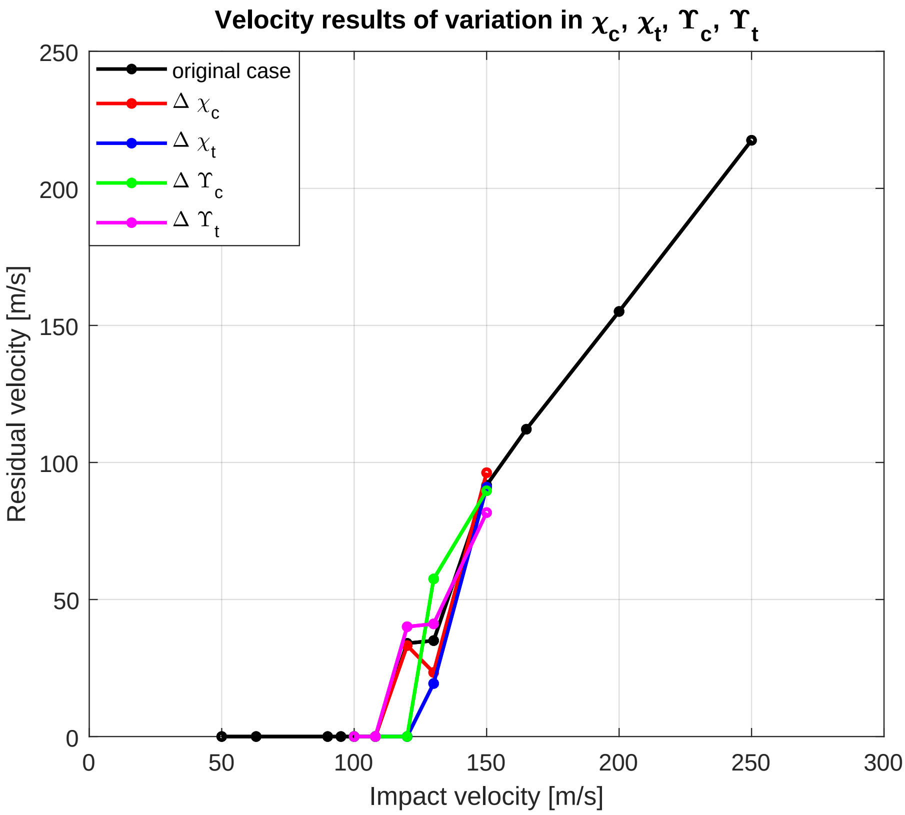


Figure 40: Comparison of delaminated area between plates with different mechanical properties

Looking now at figure 41, the differences are more observable. As in previous graph, only velocity points around the ballistic limit are plotted. It is noticeable that increasing the cohesive properties (red) shifts the ballistic limit towards the left, so it penetrates earlier. The effect of increasing these properties makes better the delamination i.e. the delamination failure is reduced considerably (as it will be seen on figure 43) in counterpart of other failure modes as it is the case of fibre breakage what eases the penetration. Moreover, increasing the shear (green) also gets the same effect although is not so noticeable in this case as with the cohesive one. Penetration is highly related to the shear, so increasing this parameter, increases also the failure of the laminate and penetration occurs earlier. On the other hand, increasing the density of the material (blue), delays the penetration what is consistent since the material gets heavier and it is more difficult to go through it.

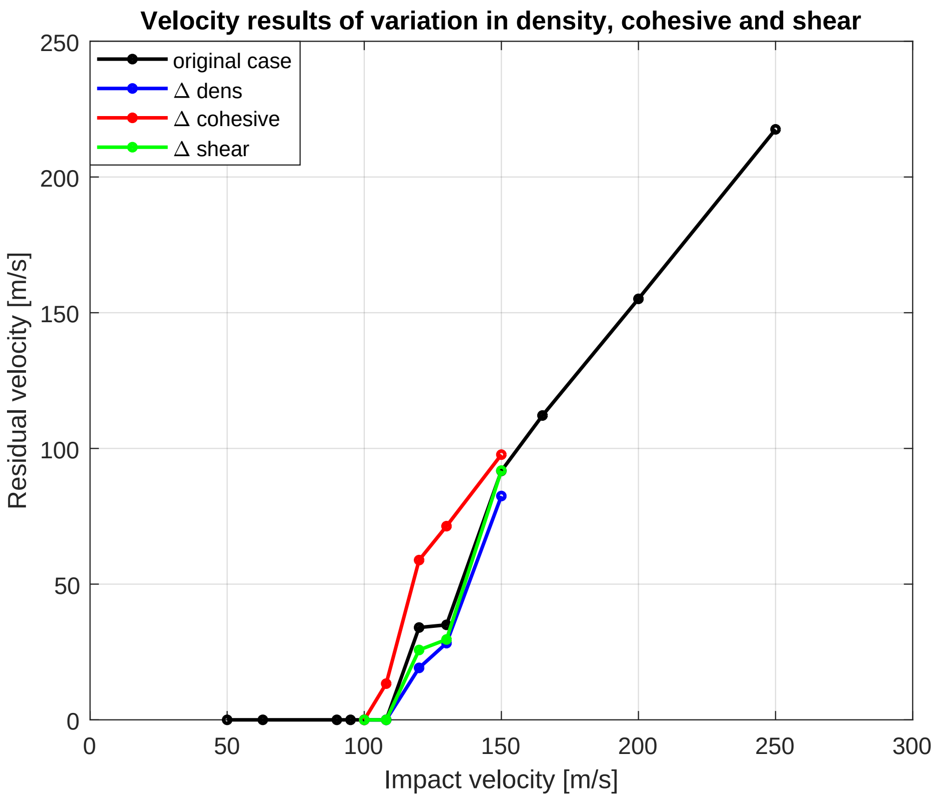


Figure 41: Comparison of delaminated area between plates with different mechanical properties

Delamination results of the variation of each type of strengths are shown in figure 42. Variations in longitudinal strengths (blue and red) show roughly the same results and the difference with respect to the original case is not so large. Tensile strength (blue) displays a bit more delamination than the compressive one (red) because the laminas tend to detach in the same direction of the fibres are oriented to.

On the other hand, transverse strengths (green and pink) show greater differences. Specifically the compressive one (green) displays a big delamination peak at the ballistic limit, meanwhile the tensile strength (pink) shows the opposite behaviour, registering the lowest results with respect to the remaining cases. In this case, this phenomenon can be explained well with figure 9 shown in the failure modes section. Matrix cracking displaces the laminas inwards so the laminas are detached. Therefore, it eases the delamination failure and this is influenced more by the compressive strength than by the tensile one. It is noticeable than depending on which parameter is studied compressive and tensile strengths have different impacts.

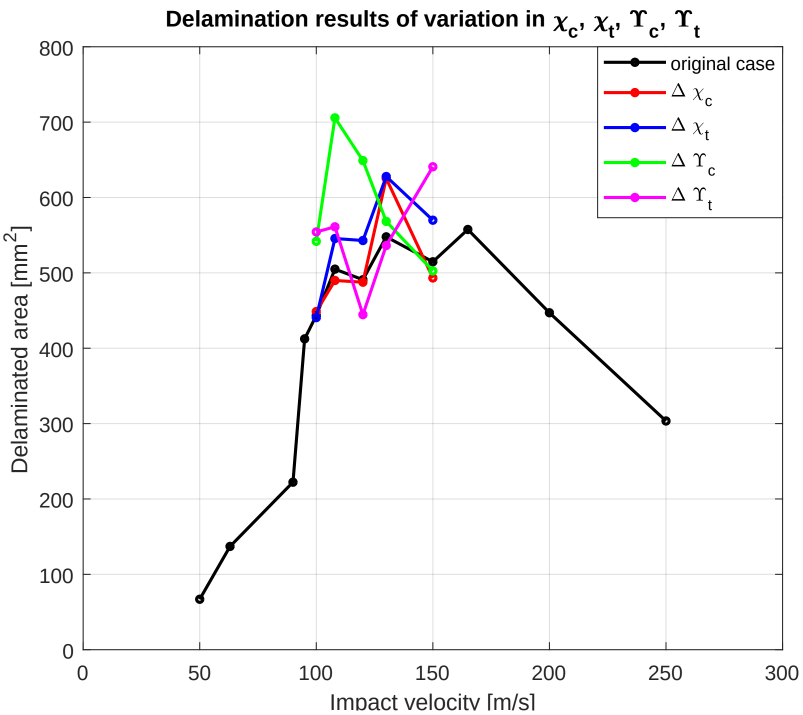


Figure 42: Comparison of residual velocities between plates with different mechanical properties

Delamination results of variations in density, cohesive and shear are displayed in figure 43. As it was explained in the velocity graph, the denser the plate, the lower the penetration. It makes the plate more compact so the delamination decreases (blue). Increasing shear (green) shows the greatest values which makes sense. Increasing the in-plane shear displaces the laminas from each other, provoking their detachment and therefore increasing the delamination. However, increasing the cohesive properties (red), improves the delamination mechanisms so the results are completely much lower than all the cases analyzed previously. In this case the delamination failure is the mode that represents the lowest results which is consistent. The failure of the material here would be induced by other types of intralaminar failure modes as it was explained within the subsection 1.3.3.

To sum up this final case, several conclusions can be extracted:

Referring to the variations in strengths, the longitudinal compressive and the transverse tensile strengths provoke the penetration earlier. However, longitudinal tensile and transverse compressive strengths eases the delamination.

On the other hand, variations in density, shear and cohesive properties have an immediately effect on both velocity and delamination results. A denser plate makes more difficult the penetration and the laminas are not so detached since are more compact. Better cohesive properties almost avoid the failure by delamination although the fibres and matrix break earlier. However, increasing shear shows bad results since the penetration occurs earlier and laminas detaches easier.

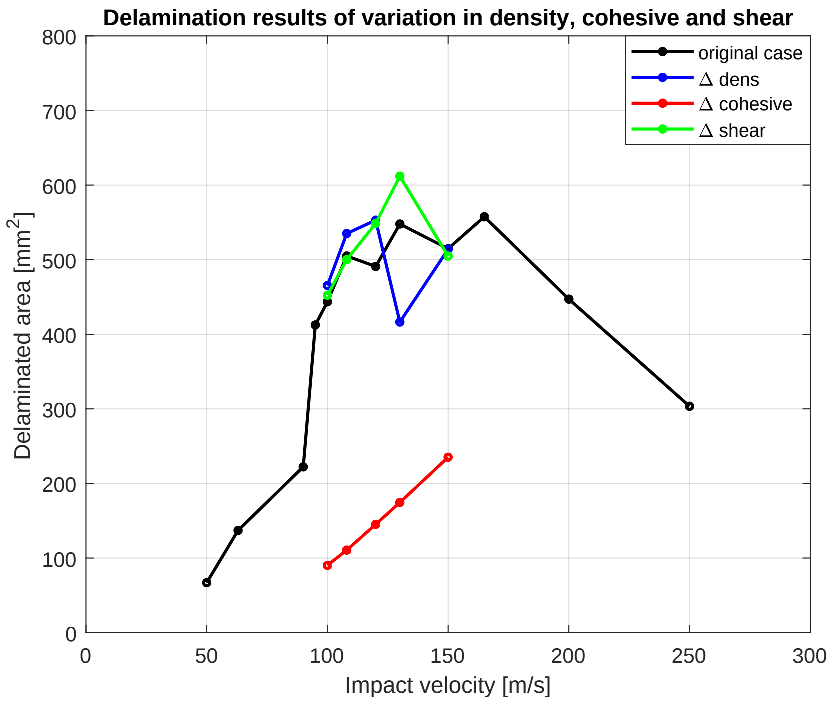


Figure 43: Comparison of residual velocities between plates with different mechanical properties

# 5 Regulatory framework

On this field there exist no regulation that may be applied since all this analysis is based on numerical simulations belonging to a scientific investigation framework.

Nevertheless, from the commercial perspective, there exist several legal stages that encompass all the agents that take part in the manufacturing, integration and certification process of composite materials in the aerospace sector.

Firstly, the supplier company is the one that provides and produces the composite product according to the demand of the major aerospace manufacturer and must supply all the data sheet of the product fulfilling with all the quality standards that the contracting company demands.

Secondly, the major manufacturer as Airbus or Boeing, is the one that utilizes the supplied composites to integrate them on their own aerospace structures. Those parts or structures built with those materials have to be tested in advance. Afterwards, the experimental results have to be satisfactory and approved in terms of security by the EASA (European Aviation Safety Agency) or any other competent authority.

Finally, these authorities are in charge of issuing all the standards and regulations based on composites materials which have to be assumed by all the aerospace companies involved. Regarding to this project, EASA establishes those enhancements to the requirements in terms of safety, such as exhaustive inspections to the aircrafts, better damage tolerance evaluations by controlling the fatigue and residual static strengths of the materials [28]. Moreover, this agency in collaboration with other global institutions as the Civil Aviation Authority, are obliged to update certification specifications regarding to composite materials [29]. Also in terms of maintenance they agree to establish any approval regarding the airworthiness management [30].

Composites still represent an unclear sector that is in continuous development. This type of materials are distinct from metallic ones and its complex behaviour makes very difficult standardize its features and characteristics. Nowadays the rules that try to regulate composites are unclear and sometimes led to inconsistent interpretations. For that reason, surely in a few years this regulatory framework will have changed and it will evolve to a more complete and uniform one.

# 6 Socio-economic environment

In this section several perspectives are going to be presented with the purpose of giving to this project both economical and social characters. After that, the budget of the whole project will be estimated, giving a segregated view of the costs involved.

## 6.1 Socio-economic impact

On one hand, this project has been done basically with computational tools. Nowadays FEM analysis represent an important part in engineering, above all for the aerospace sector as it is in this project. It is possible to model and test almost every type of material in every part of the aircraft by spending hours of simulations but without wasting money on real models and prototypes until the analyzed data show a satisfying outcome. Therefore, as it will be presented later on the budget section, the majority of the budget of this project is based on simulations and not in experimental testing.

On the other hand, computational simulations also gives the chance to expand the knowledge by analyzing and knowing an infinite number of potential candidates of composites and new materials to be used on the aerospace industry. This project also aims to contribute to the series of analysis based on ballistic impacts that have been realized continuously for many years by worldwide important companies that have become a reference in the sector.

By doing all these investigations and analysis, it is possible to change the idea that the human being has about the means of transport, specially for the case of the aerospace one. Maybe thanks to tests and simulations like these, aircrafts, satellites, rockets and space shuttles will evolve to more aerodynamically efficient ones, with materials much lighter, even transparent, unbreakable, resistant to any type of impacts and conditions, without generating any noise nor pollution and therefore saving fuel and investing in new ways of combustion much powerful but at the same time ”environmentally friendly”.

But not only the aerospace and transport sectors will be influenced by the developing of new types of composites. These materials are present in almost every object of the daily life of people. From the clothes that people wear to the chemical products used for cleaning, composites will contribute to create shirts, jeans, protective goggles and gloves with fibres resistant to hard conditions as they would encounter in atmosphere or space. Security departments as Police and army will develop better bulletproof vest and the construction industry will evolve and use bricks and materials that will create the next generation of houses, energetically more efficient and ecological.

## 6.2 Project budget

In this section it is going to be mentioned the estimation of the budget associated to the realization of this thesis.

Firstly, the price of all the software used is estimated. To realize all the simulations of each case, LS-Dyna® has been installed including all the processors and subprograms as LSPrePost®. According to Predictive Engineering FEM consulting, the price of the complete installation of LS-Dyna is about 6000 $ which is equivalent to 5300 €. Nevertheless, the University posses the licence for academic purposes with a price of 1000 €. Since the realization of the thesis has lasted around 6 months the license cost will be the half of the original price.

Alternatively, *ImageJ* was used as image processing tool to calculate the area of the delamination associated to each impact test. By counting the pixels "damaged" then they will be converted to $mm^2$. In any case, the license cost of this program is 0 €since the installation is free and available online.

Lastly, *Matlab R2017b student version* and *Microsoft Office 365* were used to collect and store all the data generated by the simulations and make all the graphics, images, calculus and statistics of the project. For the first one, since its purpose is for academic use, its license costs 69 €meanwhile the second one has a price of 125 €.

Secondly the personnel involved in this thesis also has an associated cost. Assuming that a junior annual salary in Spain is about 21500 €, it represents a salary of about 10.35 €per working hour [31]. It has been made around 330 different cases throughout this project, including those used in the sensitivity analysis to determine the correct meshes, which stands for an average of 12 velocity impacts per case. Since one simulation lasts an average of 90 min in generating all the files, the total computation time of this project is over 550 hours so the total time devoted to the overall thesis is over 650 hours. Thus, the personnel expenses are 6750 €.

It is noticeable including also in these expenses the salary of the tutor. Including all the meeting hours, emails and conversations that stands for 30 hours and assuming a salary of 20 €/hour, the supervisor cost is 600 €. Thereby the personnel expenses arise to 7350 €and the total budget of the project is about 8044 €.

| Software cost | | | |
|---|---|---|---|
| Computational Tool | Type of license | Time | Total cost |
| LS-Dyna® | annual | 6 months | 500 € |
| Matlab R2017b student version | annual | 6 months | 69 € |
| Microsoft Office 365 | permanent | 6 months | 125 € |
| ImageJ | permanent | 6 months | 0 € |
| Personnel expenses | | | |
| Personal | Dedication | Time cost | Total cost |
| Junior engineer (student) | 650 hours | 10.35 €/hour | 6750 € |
| Tutor (supervisor) | 30 hours | 20 €/hour | 600 € |
| Total project budget | | | 8044 € |

Table 9: Segregated costs and expenses of the total budget

# 7 Conclusions

## 7.1 Final conclusions

This project aims to analyze different composite laminate plate models which have been subjected to ballistic impacts. To sum up all the results obtained during the simulations, the following conclusions can be extracted:

- The simulations performed with this computational modelling tool called LS-Dyna® throughout all this project, show a notable similarity as it was observed in the results of the sensitivity analysis. Both delamination and velocity tests are very reliable which indicates that the formulation, equations and models implemented in the selected options of the computational tool are correct and so close to the real behaviour of a composite laminate plate subjected to ballistic impact.

- There exist some differences in delamination results varying the shape of the laminate plate but it can be stated that those variations are not significant since the error between the cases analyzed are not dramatic and the same behaviour is plotted in all the cases.

  In terms of velocity results, no noticeable differences are highlighted, so finally it can be stated that this initial conditions about the dimensional variations have no effect on the parameters studied.

- The thicker the laminate plate is (the more laminas is composed of), the less delaminated area is generated before the ballistic limit is reached. Once the penetration is performed after the impact, delamination increases as the velocity does, since the material is composed of more laminas.

  The thicker the laminate plate is, the more resistant is to the impact. There are more laminas to go through, so the residual velocity decreases as the impact velocity increases.

  For this reason, in order to improve delamination and reduce the residual velocity of the impact, increasing the thickness of the laminate plate plays a very important role.

- Variation in bc´s has no such a big influence as it might be thought in advance. Delamination results show that the type of constraint implemented on the boundary plate does not matter since the area between the cases is slightly the same with the only difference of the free case, which represent the largest results.

  On the other hand, the implementation of one or another type of boundary condition has no effect on the residual velocity.

  This is consistent and related to the dimensional variations. Boundary and initial conditions have no important influence on the failure of the material and residual velocity, although they are difficult to estimate since they depends on the scenarios that are going to be tested.

- Varying the longitudinal/transverse compressive/tensile strengths have different effects on the residual velocity and on the delamination failure. On one hand the longitudinal compressive and the transverse tensile strengths provoke the rupture of the fibres and the matrix cracking respectively so penetration occurs earlier. On the other hand, related to the delamination failure, the remaining respective strengths influence more than previous two. Longitudinal tensile and transverse compressive strengths eases the detachment of the laminas so the delamination is greater.

  On the other hand increasing the density of the material, makes the plate more resistant to impact and increases the compactness so both residual velocity and area delaminated decrease. Increasing the cohesive properties improves the delamination modelling so the area decreases considerably, but eases the appearance of other intralaminar failure modes as fibre/matrix breakage. Finally, increasing the shear eases the detachment of laminas, therefore the delamination and even penetration occurs earlier so it represents a bad behaviour in this analysis.

## 7.2 Future work

After the realization of this project, it is possible to continue developing the analysis of ballistic impacts in composites including new possibilities of analysis.

Firstly, performing the experimental tests of all the cases done in this project with the purpose of confirming all the results obtained through computational simulations.

Secondly, increasing the cases to be analyzed on the section of variation of the plate thickness. Once done this, it could be possible to determine an equation that may relate the area delaminated with the number of laminas.

Finally, giving another scope of work, it could be possible to realize simulations of hyper-velocity impacts on different materials, preferably those utilized on satellites and space components. It would be compared with data of real cases in which space shuttles received impacts of debris of disable satellites or any other components of space rockets which encompass the also called ”space junk”.

# References


[1] INECO. *Jornada sobre demanda de transporte aéreo*. Tech. rep. Universidad Politécnica de Madrid, Jan. 2009. URL: http://oa.upm.es/5776/1/INVE_MEM_2009_72861.pdf (visited on 01/20/2019).

[2] J. Hale. "Boeing 787 from the Ground Up". In: (), pp. 4–5. URL: https://www.boeing.com/commercial/aeromagazine/articles/qtr_4_06/AERO_Q406_article4.pdf (visited on ).

[3] AIRBUS. *Composites: Airbus continues to shape the future*. Airbus. Aug. 2017. URL: https://www.airbus.com/newsroom/news/en/2017/08/composites--airbus-continues-to-shape-the-future.html.

[4] J.J. Fernández. *Protección balística y frente a impactos en aeronave*. 2018.

[5] J. Lloret. *Introduction to Air Navigation*. Second edition. Createspace Independent Pub, 2016.

[6] J.N. Reddy. *Mechanics of Laminated composite plates and shells*. Second edition. CRC Press, 2004.

[7] S. Milenkovic. *Topic 10. Composite materials I*. online. 2015.

[8] S. K. García Castillo. *Análisis de laminados de materiales compuestos con precarga en su plano y sometidos a impactos*. 2007.

[9] J. Martín Montal. *Study of the ballistic limit of carbon fiber laminates throughout MEF and neural networks methodologies combined*. Jan. 2016.

[10] S. Milenkovic. *Topic 10. Composite materials II*. online. 2015.

[11] *HexPly® 8552 Product Data Sheet*. Data Sheet. Hexcel®, 2016.

[12] J. Pernas. "Análisis y simulación de impactos de hielo sobre laminados carbono/epoxi". PhD thesis. Universidad Carlos III de Madrid, 2013.

[13] A.H. Ziadoon and Z. Chwei. "Effect the stacking sequences of composite laminates under low velocity impact on failure modes by using carbon fiber reinforced polymer". In: *The International Journal Of Engineering And Science* 5 (Feb. 2016). URL: http://www.theijes.com/papers/v5-i2/Version-2/H05202053060.pdf.

[14] Abrate S. "Impact on Laminated Composites: Recent Advances". In: *Applied Mechanics Reviews - APPL MECH REV* 47 (Nov. 1994). DOI: 10.1115/1.3111065.

[15] W. J. Cantwell and J. Morton. *Comparison of the low and high velocity impact response of CFRP*. Vol. 20. Composites. Nov. 1989.

[16] J. Santos. *Análisis paramétrico de impactos de alta velocidad contra laminados de material compuesto mediante FEM*. Oct. 2018.

[17] Derek Hull and Yi Bing Shi. "Damage mechanism characterization in composite damage tolerance investigations". In: *Composite Structures* 23.2 (1993), pp. 99–120. ISSN: 0263-8223. DOI: https://doi.org/10.1016/0263-8223(93)90015-I. URL: http://www.sciencedirect.com/science/article/pii/026382239390015I.

[18] O Allix and Alberto Corigliano. "Modeling and simulation of crack propagation in mixed-modes interlaminar fracture specimens". In: *International Journal of Fracture* 77 (Jan. 1996), pp. 111–140. DOI: 10.1007/BF00037233.

[19] Kurt Henkhaus and Guillermo Ramirez. "OVERVIEW OF RESEARCH ON COMPOSITE MATERIAL IMPACT BEHAVIOR". In: (Mar. 2019).

[20] Rahul Reddy Nagavally. "Composite Materials - History, Types, Fabrication Techniques, Advantages, and Applications". In: *International Journal of Mechanical and Production Engineering, IJMPE* 5 (2017), pp. 82–87.

[21] J. Hult and F.G. Rammerstorfer. *Engineering Mechanics of Fibre Reinforced Polymers and Composite Structures*. CISM International Centre for Mechanical Sciences. Springer Vienna, 2014. ISBN: 9783709127025. URL: https://books.google.es/books?id=oN5sCQAAQBAJ.

[22] "Determination of Ballistic Limit for IM7/8552 Using LS-DYNA MAT 261". In: AIRCRAFT DESIGN, TESTING AND PERFORMANCE (2018). URL: https://ntrs.nasa.gov/search.jsp?R=20180006199.

[23] Hyung Yun Choi and Fu-Kuo Chang. "A Model for Predicting Damage in Graphite/Epoxy Laminated Composites Resulting from Low-Velocity Point Impact". In: *Journal of Composite Materials* 26.14 (1992), pp. 2134–2169. DOI: 10.1177/002199839202601408. URL: https://doi.org/10.1177/002199839202601408.

[24] LC Lin and A Bhatnagar. "Ballistic Energy Absorption of Composites II". In: *Advanced Materials-Affordable Processes* 23 (1991), pp. 669–683.

[25] *LS-DYNA® KEYWORD USER'S MANUAL VOLUME I LS-DYNA R10.0*. LIVERMORE SOFTWARE TECHNOLOGY CORPORATION (LSTC), 2017. URL: https://www.dynasupport.com/manuals/ls-dyna-manuals/ls-dyna-manual-r10.0-vol-i.

[26] *LS-DYNA® KEYWORD USER'S MANUAL VOLUME II Material Models LS-DYNA R10.0*. LIVERMORE SOFTWARE TECHNOLOGY CORPORATION (LSTC), 2017. URL: https://www.dynasupport.com/manuals/ls-dyna-manuals/ls-dyna-manual-r10.0-vol-ii.

[27] fu-kuo Chang and Kuo-Yen Chang. "A Progressive Damage Model for Laminated Composites". In: *Journal of Composite Materials - J COMPOS MATER* 21 (Sept. 1987), pp. 834–855. DOI: 10.1177/002199838702100904.

[28] EXECUTIVE DIRECTOR OF THE EUROPEAN AVIATION SAFETY AGENCY. *European Aviation Safety Agency: Certification Specifications for Large Rotorcraft ('CS-29')*. Decision 2012/022/R. Dec. 2012. URL: https://www.easa.europa.eu/sites/default/files/dfu/ED%5C%20Decision%5C%202012-022-R.pdf.

[29] *EASA website*. [Online]. URL: https://www.easa.europa.eu/the-agency/the-agency (visited on 03/13/2019).

[30] *Civil Aviation Authority website*. [Online]. URL: https://www.caa.co.uk/home/ (visited on 01/14/2019).

[31] *Junior Engineer Salaries in Spain*. [Online]. URL: https://www.glassdoor.com/Salaries/madrid-junior-engineer-salary-SRCH_IL.0,6_IM1030_KO7,22.htm (visited on 02/09/2019).

# Appendix A
# Ballistic impact modelling code of LS-Dyna®

***$# LS-PrePost command file created by LS-PrePost(R) V4.5.21 - 31May2018 -64bit-Window***

***$# Created on Mar-07-2019 (13:21:48) by Alberto Rodriguez Amor***

***openc keyword "C:\Users\Alberto\Documents\LS-DYNA\TFG\ejemplostfg\ejemplos8pliegues\110x110mm***

***\placa110x110mmveloc100ms.k"***

***save keywordoutversion 9***

**KEYWORD INPUT 1**

meshing boxsolid create 0.000000 0.000000 0.000000 165.000000 110.000000 0.200000 165 110 1 0.000000 ac

meshing boxsolid accept 1 1 1 45d genselect clear
ac

meshing boxsolid create 0.000000 0.000000 0.200000 165.000000 110.000000 0.400000 165 110 1 0.000000 ac

meshing boxsolid accept 2 18151 36853 -45d genselect clear
ac

meshing boxsolid create 0.000000 0.000000 0.400000 165.000000 110.000000 0.600000 165 110 1 0.000000 ac

meshing boxsolid accept 3 36301 73705 0d genselect clear
ac

meshing boxsolid create 0.000000 0.000000 0.600000 165.000000 110.000000 0.800000 165 110 1 0.000000 ac

meshing boxsolid accept 4 54451 110557 90d genselect clear
ac

meshing boxsolid create 0.000000 0.000000 0.800000 165.000000 110.000000 1.000000 165 110 1 0.000000 ac

meshing boxsolid accept 5 72601 147409 90u genselect clear
ac

meshing boxsolid create 0.000000 0.000000 1.000000 165.000000 110.000000 1.200000 165 110 1 0.000000 ac

meshing boxsolid accept 6 90751 184261 0u genselect clear
ac

meshing boxsolid create 0.000000 0.000000 1.200000 165.000000 110.000000 1.400000 165 110  1 0.000000 ac

meshing boxsolid accept 7 108901 221113 -45u genselect clear
ac

meshing boxsolid create 0.000000 0.000000 1.400000 165.000000 110.000000 1.600000 165 110  1 0.000000 ac

meshing boxsolid accept 8 127051 257965 45u genselect clear
ac

meshing spheresolid create 55 55 6 3.75 4 1 0 0 0 1 0

***BOUNDARY_SPC_SET_ID**

$#     id                                                  heading

*clamped*

$#   nsid     cid     dofx     dofy     dofz     dofrx     dofry     dofrz

1     0     1     1     1     1     1     1

***CONTACT_AUTOMATIC_SURFACE_TO_SURFACE**

$#     cid                                                  title

$#   ssid     msid     sstyp     mstyp   sboxid   mboxid     spr     mpr

16     15     0     0     0     0     0     0

$#     fs     fd     dc     vc     vdc   penchk     bt     dt

0.0     0.0     0.0     0.0     0.0     0     0.0     1.00000E20

$#     sfs     sfm     sst     mst     sfst     sfmt     fsf     vsf

1.0     1.0     0.0     0.0     1.0     1.0     1.0     1.0

$#   soft   sofscl   lcidab   maxpar   sbopt   depth   bsort   frcfrq

2     0.1     0     1.025     2.0     2     0     1

keyword updatekind

***CONTACT_AUTOMATIC_SURFACE_TO_SURFACE_TIEBREAK**

$#     cid                                                  title

$#   ssid     msid     sstyp     mstyp   sboxid   mboxid     spr     mpr

1     2     0     0     0     0     1     1

```
$#     fs       fd       dc       vc      vdc   penchk       bt       dt
      0.0      0.0      0.0      0.0      0.0        0      0.01.00000E20
$#    sfs      sfm      sst      mst     sfst     sfmt      fsf      vsf
      1.0      1.0      0.0      0.0      1.0      1.0      1.0      1.0
$# option     nfls     sfls    param   eraten   erates    ct2cn       cn
         9     40.0     64.0    -1.45     0.25     0.75     0.75  40000.0
*SET_SEGMENT_TITLE
45º
$#    sid      da1      da2      da3      da4   solver
                   1      0.0      0.0      0.0      0.0MECH
$#     n1         n2        n3        n4      a1       a2       a3       a4
   24592   24591   24480   24481      0.0      0.0      0.0      0.0
   24337   24336   24225   24226      0.0      0.0      0.0      0.0
   24082   24081   23970   23971      0.0      0.0      0.0      0.0
   23827   23826   23715   23716      0.0      0.0      0.0      0.0
   23572   23571   23460   23461      0.0      0.0      0.0      0.0
*SET_SEGMENT_TITLE
-45º
$#    sid      da1      da2      da3      da4   solver
                 2      0.0      0.0      0.0      0.0MECH
$#     n1         n2        n3        n4      a1       a2       a3       a4
   36720   36831   36832   36721      0.0      0.0      0.0      0.0
   36465   36576   36577   36466      0.0      0.0      0.0      0.0
   36210   36321   36322   36211      0.0      0.0      0.0      0.0
   35955   36066   36067   35956      0.0      0.0      0.0      0.0
   35700   35811   35812   35701      0.0      0.0      0.0      0.0
   35445   35556   35557   35446      0.0      0.0      0.0      0.0
   35190   35301   35302   35191      0.0      0.0      0.0      0.0
```

***SET_SEGMENT_TITLE**

*0º*

```
$#    sid      da1      da2      da3      da4    solver
                  11      0.0      0.0      0.0      0.0MECH
$#       n1          n2       n3             n4       a1       a2       a3       a4
   221000   220999   220833   220834      0.0      0.0      0.0      0.0
   220745   220744   220578   220579      0.0      0.0      0.0      0.0
   220490   220489   220323   220324      0.0      0.0      0.0      0.0
   220235   220234   220068   220069      0.0      0.0      0.0      0.0
   219980   219979   219813   219814      0.0      0.0      0.0      0.0
```

***SET_SEGMENT_TITLE**

*90º*

```
$#    sid      da1      da2      da3      da4    solver
                   9      0.0      0.0      0.0      0.0MECH
$#       n1       n2             n3          n4       a1       a2       a3       a4
   184024   184023   183857   183858      0.0      0.0      0.0      0.0
   183769   183768   183602   183603      0.0      0.0      0.0      0.0
   183514   183513   183347   183348      0.0      0.0      0.0      0.0
   183259   183258   183092   183093      0.0      0.0      0.0      0.0
   183004   183003   182837   182838      0.0      0.0      0.0      0.0
   182749   182748   182582   182583      0.0      0.0      0.0      0.0
```

***SET_SEGMENT_TITLE**

*ball*

```
$#    sid      da1      da2      da3      da4    solver
                  17      0.0      0.0      0.0      0.0MECH
```

$#     n1           n2       n3             n4       a1       a2       a3       a4

197920  197884  197878  197914  0.0  0.0  0.0  0.0

197883  197889  197890  197884  0.0  0.0  0.0  0.0

197883  197884  197920  197919  0.0  0.0  0.0  0.0

197885  197816  197922  197921  0.0  0.0  0.0  0.0

197575  197630  197666  197665  0.0  0.0  0.0  0.0

197921  197885  197879  197915  0.0  0.0  0.0  0.0

197666  197630  197624  197660  0.0  0.0  0.0  0.0

197884  197890  197891  197885  0.0  0.0  0.0  0.0

***SET_SEGMENT_TITLE**

*plate*

$#    sid      da1      da2      da3      da4    solver

15      0.0      0.0      0.0      0.0MECH

$#     n1      n2      n3      n4      a1      a2      a3      a4

65280  71496  71497  65281  0.0  0.0  0.0  0.0

65025  71241  71242  65026  0.0  0.0  0.0  0.0

64770  70986  70987  64771  0.0  0.0  0.0  0.0

64770  64826  64827  64771  0.0  0.0  0.0  0.0

64260  70476  70477  64261  0.0  0.0  0.0  0.0

64260  64316  64317  64261  0.0  0.0  0.0  0.0

***CONTROL_TERMINATION**

$#endtim    endcyc    dtmin    endeng    endmas    nosol

2.50000E-4       0      0.0      0.01.000000E8       0

*END

***INITIAL_VELOCITY_GENERATION**

$#nsid/pid     styp    omega       vx       vy       vz             ivatn     icid

9       2      0.0      0.0      0.0   -100000.0       0       0

```
$#     xc       yc       zc       nx       ny       nz    phase   irigid
      0.0      0.0      0.0      0.0      0.0      0.0       0        0
*END
```

***PART**

```
$#                                                   title    ball
$#    pid    secid     mid    eosid     hgid     grav   adpopt     tmid
           9       1          1       0          0        0             0        0
```

***SECTION_SOLID**

```
$#   secid   elform      aet
         1          1       0
```

***MAT_ENHANCED_COMPOSITE_DAMAGE_TITLE**

*45º*

```
$#    mid       ro                ea             eb           (ec)     prba       (prca)   (prcb)
                21.58000E-9  139000.0    9000.0    9000.0   0.01996      0.0      0.0
$#    gab      gbc      gca     (kf)     aopt     2way
   5000.0    4500.0   4500.0      0.0      2.0      0.0
$#     xp       yp       zp       a1       a2       a3   mangle
      0.0      0.0      0.0      1.0      1.0      0.0      0.0
$#     v1       v2       v3       d1       d2       d3   dfailm   dfails
        0.0      0.0      0.0      0.0      1.0      0.0     0.04     0.04
$#   tfail     alph     soft     fbrt    ycfac   dfailt   dfailc      efs
        0.0      0.0      1.0      0.0      2.0     0.04    -0.04     0.15
$#     xc            xt          yc       yt           sc     crit     beta
     1656.0   2105.0   175.0     79.0   114.0     54.0      0.0
$#    pel       epsf     epsr     tsmd    soft2
          0.0      0.0      0.0       0.0      1.0
```

$# slimt1 slimc1 slimt2 slimc2 slims ncyred softg

0.0 0.0 0.0 0.0 0.0 0.0 1.0

*END

***MAT_ENHANCED_COMPOSITE_DAMAGE_TITLE**

*-45º*

$# mid ro ea eb (ec) prba (prca) (prcb)

31.58000E-9 139000.0 9000.0 9000.0 0.01996 0.0 0.0

$# gab gbc gca (kf) aopt 2way

5000.0 4500.0 4500.0 0.0 2.0 0.0

$# xp yp zp a1 a2 a3 mangle

0.0 0.0 0.0 1.0 -1.0 0.0 0.0

$# v1 v2 v3 d1 d2 d3 dfailm dfails

0.0 0.0 0.0 0.0 1.0 0.0 0.04 0.04

$# tfail alph soft fbrt ycfac dfailt dfailc efs

0.0 0.0 1.0 0.0 2.0 0.04 -0.04 0.15

$# xc xt yc yt sc crit beta

1656.0 2105.0 175.0 79.0 114.0 54.0 0.0

$# pel epsf epsr tsmd soft2

0.0 0.0 0.0 0.0 1.0

$# slimt1 slimc1 slimt2 slimc2 slims ncyred softg

0.0 0.0 0.0 0.0 0.0 0.0 1.0

*END

***MAT_ENHANCED_COMPOSITE_DAMAGE_TITLE**

*0º*

$# mid ro ea eb (ec) prba (prca) (prcb)

41.58000E-9 139000.0 9000.0 9000.0 0.01996 0.0 0.0

```
$#    gab      gbc           gca     (kf)     aopt     2way
   5000.0   4500.0   4500.0      0.0      2.0      0.0
$#     xp       yp       zp       a1       a2       a3    mangle
      0.0      0.0      0.0      1.0      0.0      0.0      0.0
$#     v1       v2       v3       d1       d2       d3    dfailm    dfails
      0.0      0.0      0.0      0.0      1.0      0.0     0.04     0.04
$#   tfail     alph     soft     fbrt    ycfac   dfailt   dfailc      efs
        0.0      0.0      1.0      0.0      2.0     0.04    -0.04     0.15
$#     xc       xt               yc       yt       sc          crit     beta
   1656.0   2105.0    175.0     79.0    114.0     54.0      0.0
$#    pel      epsf     epsr     tsmd     soft2
         0.0      0.0      0.0      0.0      1.0
$#  slimt1    slimc1    slimt2    slimc2    slims    ncyred    softg
        0.0      0.0        0.0        0.0       0.0      0.0        1.0
*END
```

***MAT_ENHANCED_COMPOSITE_DAMAGE_TITLE**

*90º*

```
$#    mid       ro                   ea                eb          (ec)     prba      (prca)    (prcb)
                 51.58000E-9   139000.0    9000.0    9000.0   0.01996      0.0      0.0
$#    gab      gbc      gca      (kf)     aopt        2way
   5000.0   4500.0   4500.0      0.0      2.0      0.0
$#     xp       yp       zp       a1       a2       a3    mangle
      0.0      0.0      0.0      0.0      1.0      0.0      0.0
$#     v1      v2       v3       d1       d2       d3    dfailm    dfails
      0.0      0.0      0.0      1.0      0.0      0.0     0.04     0.04
```

```
$#   tfail   alph     soft     fbrt     ycfac   dfailt   dfailc      efs
     0.0      0.0      1.0      0.0      2.0     0.04    -0.04     0.15
$#     xc            xt         yc         yt         sc       crit     beta
   1656.0   2105.0    175.0     79.0    114.0     54.0      0.0
$#    pel     epsf     epsr     tsmd    soft2
        0.0      0.0      0.0      0.0      1.0
$#  slimt1    slimc1    slimt2    slimc2    slims    ncyred    softg
         0.0      0.0        0.0         0.0      0.0        0.0      1.0
*END
```

***MAT_ELASTIC_TITLE**

*elastic*

```
$#    mid      ro             e                pr        da       db     not used
            17.85000E-9    210000.0     0.33      0.0      0.0       0
*END
```

***DATABASE_BINARY_D3PLOT**

```
$#     dt              lcdt     beam     npltc    psetid
1.00000E-5         0          0            0        0
$#   ioopt
       0
*END
```

***DATABASE_BINARY_INTFOR**

```
$#     dt             lcdt     beam     npltc    psetid
1.00000E-5       0           0            0           0
$#   ioopt
       0
*END
```

***DATABASE_GLSTAT**

$# dt binary lcur ioopt

1.00000E-5 0 0 1

*END

***DATABASE_MATSUM**

$# dt binary lcur ioopt

1.00000E-5 0 0 1

*END

***save keywordabsolute 0***

***save keywordbylongfmt 0***

***save outversion***

***save keyword "C:\Users\Alberto\Documents\LS-DYNA\110x110v100.k"***

# Appendix B - 55x110 mm laminate plate

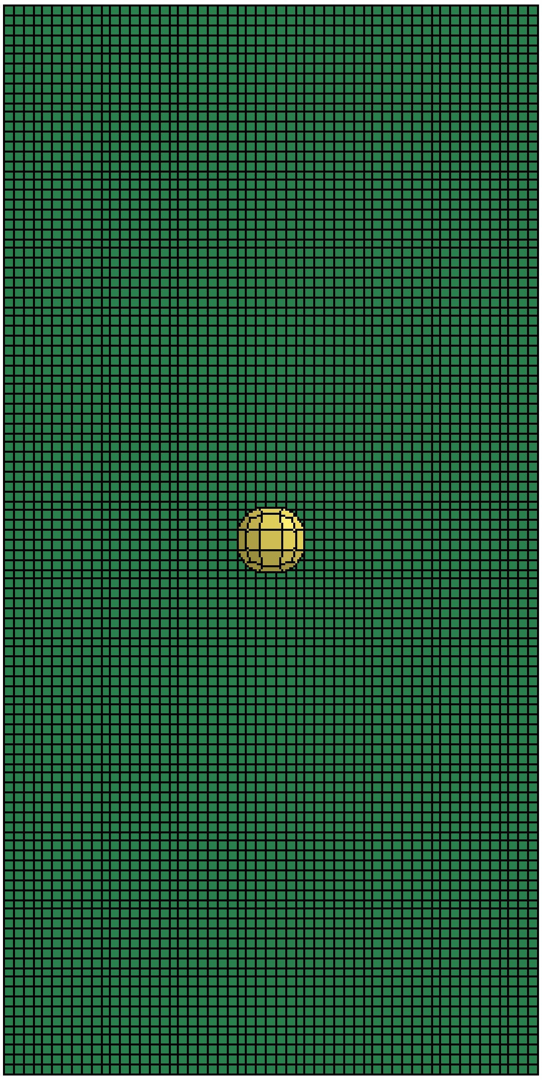

## Appendix C - 110x110 mm laminate plate

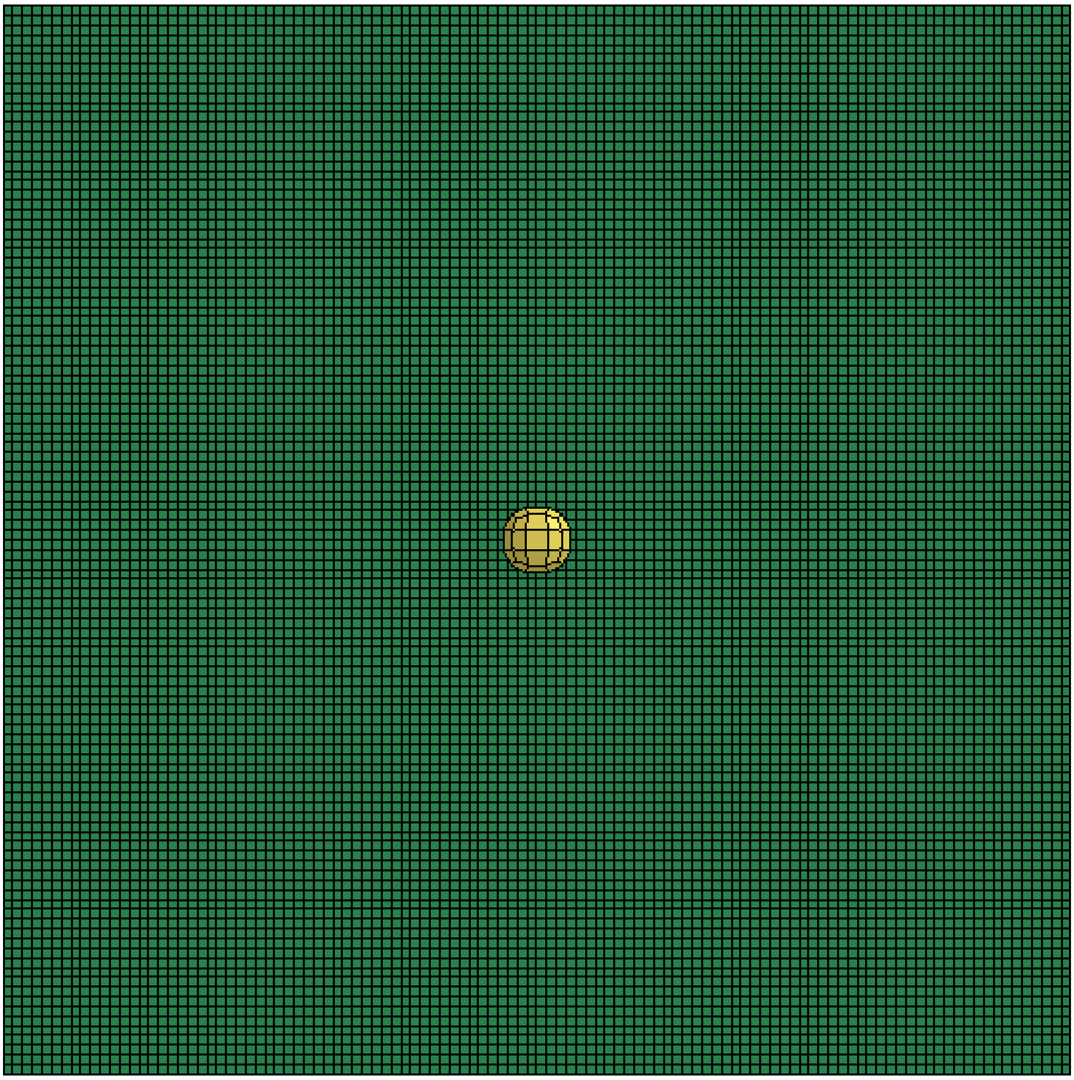

# Appendix D - 165x110 mm laminate plate

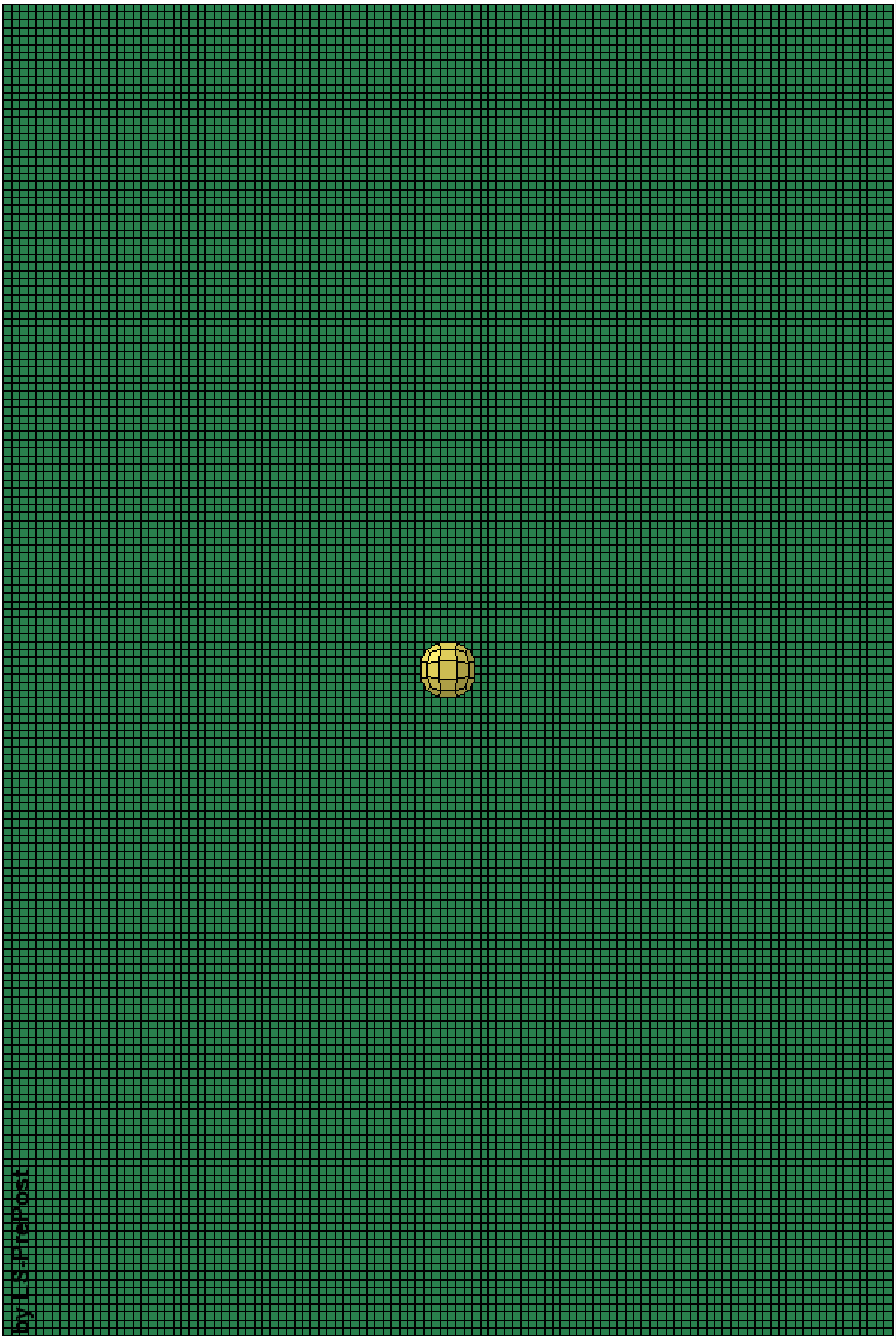

# Appendix E - Gantt Chart

## Gantt Chart

### Analysis of composite laminate plate subjected to ballistic impact

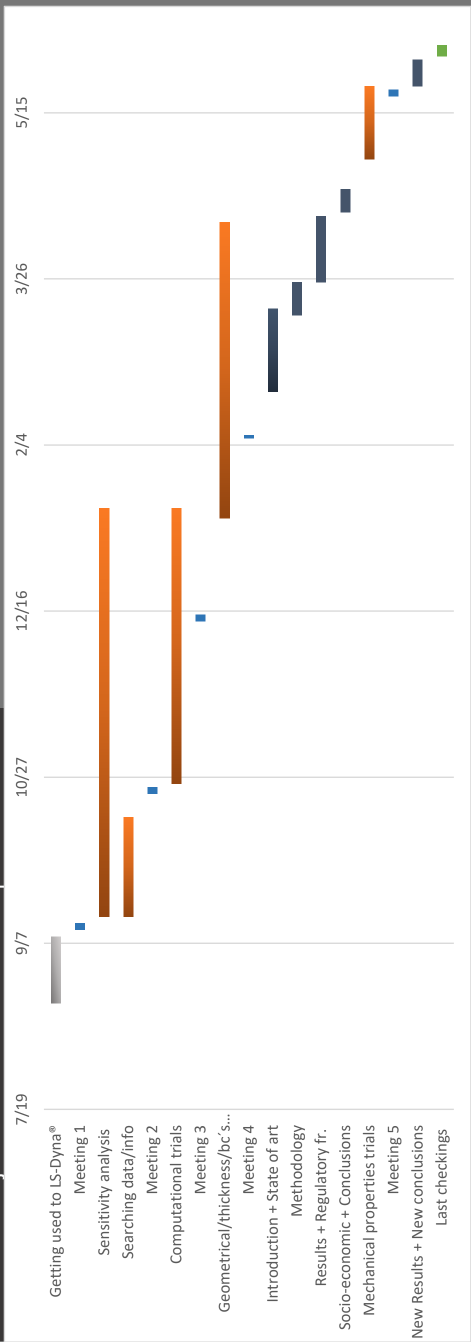


| START DATE | END DATE | DESCRIPTION | DURATION (days) |
|---|---|---|---|
| 8/20/18 | 9/10/18 | Getting used to LS-Dyna® | 20 |
| 9/11/18 | 9/13/18 | Meeting 1 | 2 |
| 9/15/18 | 1/18/19 | Sensitivity analysis | 123 |
| 9/15/18 | 10/15/18 | Searching data/info | 30 |
| 10/22/18 | 10/24/18 | Meeting 2 | 2 |
| 10/25/18 | 1/18/19 | Computational trials | 83 |
| 12/13/18 | 12/15/18 | Meeting 3 | 2 |
| 1/13/19 | 4/12/19 | Geometrical/thickness/bc´s trials | 89 |
| 2/6/19 | 2/7/19 | Meeting 4 | 1 |

| START DATE | END DATE | DESCRIPTION | DURATION (days) |
|---|---|---|---|
| 2/20/19 | 3/15/19 | Introduction + State of art | 25 |
| 3/15/19 | 3/25/19 | Methodology | 10 |
| 3/25/19 | 4/15/19 | Results + Regulatory fr. | 20 |
| 4/15/19 | 4/22/19 | Socio-economic + Conclusions | 7 |
| 5/1/19 | 5/23/19 | Mechanical properties trials | 22 |
| 5/20/19 | 5/22/19 | Meeting 5 | 2 |
| 5/23/19 | 6/1/19 | New Results + New conclusions | 8 |
| 6/1/19 | 6/10/19 | Last checkings | 9 |